Stem Cell Reports
Article

ISSCR

OPEN ACCESS

A feedforward loop between JAK/STAT downstream target p115 and STAT in germline stem cells

Ruiyan Kong,[1] Juan Li,[1] Fuli Liu,[1] Yankun Ma,[1] Hang Zhao,[1] Hanfei Zhao,[1] Meifang Ma,[1] and Zhouhua Li[1,*]
[1]College of Life Sciences, Capital Normal University, Beijing 100048, China
*Correspondence: zhli@cnu.edu.cn
https://doi.org/10.1016/j.stemcr.2023.08.007

SUMMARY

The maintenance of germline stem cells (GSCs) is essential for tissue homeostasis. JAK/STAT signaling maintains GSC fate in *Drosophila* testis. However, how JAK/STAT signaling maintains male GSC fate through its downstream targets remains poorly understood. Here, we identify p115, a tER/*cis*-Golgi golgin protein, as a putative downstream target of JAK/STAT signaling. p115 maintains GSC fate independent of GM130 and GRASP65. p115 localizes in cytosol, the ER and Golgi apparatus in germline cells and is required for the morphology of the ER and Golgi apparatus. Furthermore, depletion of p115 in GSCs results in aberrant spindle orientation. Mechanistically, p115 associates with and stabilizes STAT. Finally, ectopic expression of STAT completely restores GSC loss caused by p115 depletion. Collectively, JAK/STAT signaling and p115 form a feedforward loop to maintain male GSC fate. Our work provides new insights into the regulatory mechanism of how stem cell maintenance is properly controlled by JAK/STAT signaling.

INTRODUCTION

Tissue homeostasis is maintained by residential stem cells through the proper balance of stem cell self-renewal and differentiation. Disruption of the balance will lead to stem cell over-proliferation or stem cell loss, eventually resulting in various diseases, such as cancer and aging (Blanpain and Fuchs, 2014; Chandel et al., 2016; Morrison and Spradling, 2008). Therefore, clarifying the mechanisms of stem cell maintenance is important for understanding tissue homeostasis control and the development of potential therapeutics for human diseases.

The *Drosophila* testis provides an ideal model system to study stem cell maintenance and differentiation (Davies and Fuller, 2008; de Cuevas and Matunis, 2011; Kiger et al., 2001; Li and Xie, 2005; Tulina and Matunis, 2001). At the tip of the *Drosophila* testis, a group of somatic cells, called the hub, physically contact with two stem cell populations: germline stem cells (GSCs) and somatic cyst stem cells (CySCs) (Decotto and Spradling, 2005; Fuller and Spradling, 2007; Hardy et al., 1979; Spradling et al., 2008). About five to nine GSCs surround the hub and each GSC is encapsulated by two CySCs. The hub and CySCs serve as the niche (microenvironment) for GSC self-renewal and differentiation (de Cuevas and Matunis, 2011; Decotto and Spradling, 2005; Morrison and Spradling, 2008). And the hub serves as the niche for both GSCs and CySCs by secreting factors such as Unpaired (Upd), which activates Janus kinase-signal transducer and activator of transcription (JAK/STAT) signaling in adjacent GSCs and CySCs to regulate their maintenance (Kiger et al., 2001; Leatherman and Dinardo, 2008; Tulina and Matunis, 2001). GSCs divide asymmetrically to produce a new GSC that remains attached to the hub (self-renewal) and a daughter cell called a gonialblast (GB), which is displaced from the hub and begins to differentiate (differentiation) (Yamashita et al., 2003). The GB undergoes four rounds of incomplete transit-amplifying divisions to produce 16 interconnected spermatogonial cells followed by two rounds of meiotic divisions and spermatocyte growth (White-Cooper et al., 2000). The fusome, a germline-specific endoplasmic reticulum (ER)-like organelle, exists in GSCs and GBs as a spherical shape (called the spectrosome) and an elongated or branched shape in interconnected differentiating spermatogonial cells (Deng and Lin, 1997; Wilson, 2005). Thus, GSCs can be distinguished by the spherical-shaped spectrosome they contain and their localizations attaching to the hub.

Local signals within the hub and CySCs are essential for GSC maintenance. The JAK/STAT signaling pathway was the first found and the most important signaling pathway in the testis to regulate GSC and CySC maintenance (Kiger et al., 2001; Tulina and Matunis, 2001). The hub secretes the JAK/STAT ligand Upd to the adjacent GSCs and CySCs, which binds to the receptor, Domeless (Dome). Dome in turn activates the JAK kinase homolog Hopscotch (Hop) and the STAT homolog Stat92E by phosphorylation. The activated Stat92E (phosphorylated Stat92E, pStat92E/pSTAT) translocates into the nucleus to regulate the transcription of downstream target genes (Binari and Perrimon, 1994; Yan et al., 1996). *Stat92E* null mutant GSCs do not persist within the hub, showing that Stat92E (STAT) is directly required for GSC maintenance (Tulina and Matunis, 2001). *Zinc-finger homeodomain protein 1* (*Zfh-1*) and *chronologically inappropriate morphogenesis* (*Chinmo*) have been identified as JAK/STAT signaling downstream targets in cyst cells (Flaherty et al., 2010; Leatherman and Dinardo, 2008). The ability of CySCs to maintain GSCs is likely to be

regulated by Zfh-1 (Leatherman and Dinardo, 2008). Suppressors of cytokine signaling are highly conserved transcriptional targets of JAK/STAT signaling and negatively regulate the JAK/STAT signaling via distinct mechanisms (Arbouzova and Zeidler, 2006; Callus and Mathey-Prevot, 2002; Rawlings et al., 2004). Socs36E is expressed in the hub and CySCs, and null *Socs36E* mutant testes showed defects in the germline (Issigonis et al., 2009). However, whether additional JAK/STAT downstream targets are required for GSC maintenance and how they maintain GSC fate remain unexplored.

To search for downstream targets of JAK/STAT signaling and novel regulators for GSC maintenance and differentiation in adult testis, we utilized adenine methylase identification (Dam-ID) technology (Gutierrez-Triana et al., 2016; Southall and Brand, 2009; van Steensel and Henikoff, 2000). We identified p115 as a putative JAK/STAT downstream candidate. p115 is a membrane-tethering protein mainly located in the transitional ER (tER) sites and *cis*-Golgi vesicles (Barroso et al., 1995; Levine et al., 1996; Nelson et al., 1998; Waters et al., 1992). tER sites are ER subdomains where proteins are packaged into COPII transport vesicles and carried out of the ER to the Golgi apparatus (Barlowe et al., 1994; Orci et al., 1991). p115 can be recruited onto COPII vesicles by Rab1 and fused with the Golgi membranes (Allan et al., 2000). Depletion of p115 in *Drosophila* S2 cells led to a quantitative breakdown of Golgi stacks and strongly affected the general organization of the tER sites without effecting intracellular transport (Kondylis and Rabouille, 2003). In mammalian cells, most Golgi matrix proteins, such as p115, GM130, and giantin, are involved in the maintenance of the Golgi stacks (Shorter et al., 2002). In addition, interactions between golgins (e.g., GM130, giantin, and p115) and the GRASP family of Golgi stacking proteins (e.g., GRASP65 and GRASP55) have been reported to play important roles in maintaining the structure of the Golgi apparatus (Barr et al., 1997; Barroso et al., 1995; Linstedt and Hauri, 1993; Nakamura et al., 1995; Shorter et al., 1999). Moreover, p115 associates with γ-tubulin throughout the cell cycle and is required for the structure and function of the late mitotic spindle during mitosis (Radulescu et al., 2011). p115 is required for correct formation of the bipolar spindle in S2 cells and regulates the *Drosophila* wing epithelial tissue size by affecting Cdk1 activation (Ibar and Glavic, 2017). However, whether and how p115 functions in *Drosophila* male sGSCs are unknown.

In this study, we provide evidence that *p115* is a putative downstream target of JAK/STAT signaling and required for male GSC maintenance. Importantly, we demonstrate that p115 interacts with and stabilizes Stat92E to form a feedforward loop to maintain GSC fate. Thus, our data uncover the underlying mechanism of p115 in GSC maintenance.

RESULTS

p115 is a putative downstream target of JAK/STAT signaling in *Drosophila* testis

JAK/STAT signaling is required for the self-renewal of GSCs and CySCs (Kiger et al., 2001; Tulina and Matunis, 2001). Previous studies have identified *Zfh-1*, *Chinmo*, and *Socs36E* as downstream targets of JAK/STAT signaling in *Drosophila* testes (Callus and Mathey-Prevot, 2002; Flaherty et al., 2010; Leatherman and Dinardo, 2008). Zfh-1 and Chinmo are required for CySC self-renewal but not GSC maintenance. Socs36E is a negative regulator of the JAK/STAT signaling and plays a role in GSC maintenance (Issigonis et al., 2009). To identify new downstream targets of JAK/STAT signaling in adult testis, we utilized the Dam-ID technique to search for genome-wide binding sites of Stat92E (STAT) *in vivo* (Gutierrez-Triana et al., 2016; Southall and Brand, 2009; van Steensel and Henikoff, 2000). We performed Dam-ID in testis with activated JAK/STAT signaling by overexpressing $hop^{Tum\text{-}l}$, a constitutively active form of the *Drosophila* JAK, *hopscotch* (Hop) (Corwin and Hanratty, 1976; Hanratty and Dearolf, 1993; Harrison et al., 1995). Enriched STAT binding regions were defined by comparing STAT-Dam methylation profiles to a Dam-alone control. Dam-ID data analysis revealed binding peaks (orange dashed box regions) in the *p115* region, indicating that p115 is a putative downstream target of JAK/STAT signaling (Figure 1A). To further confirm that p115 is regulated by JAK/STAT signaling, we examined the expression levels of p115 through quantitative real-time reverse transcriptase PCR and western blot. The results showed that the expression levels of *p115* were upregulated upon activation of JAK/STAT signaling (Figure 1B). Consistently, the protein levels of p115 were also significantly increased upon JAK/STAT signaling activation (Figures 1C and 1D). Interestingly, further depletion of p115 in testes with activated JAK/STAT signaling significantly reduced the levels of *p115* transcripts and p115 proteins (Figures 1B–1D). Together, these data show that p115 is a putative downstream target of JAK/STAT signaling in testis.

p115 is required for male GSC maintenance

To examine the function of p115 in adult *Drosophila* testis, we generated a functional shRNA against *p115* (Figures 1B–1D and S1). Systemic depletion of p115 resulted in atrophic testes, indicating that p115 is essential for the full function of testis (Figures S2A and S2B). We then pinned down the cell type(s) in which p115 plays an essential role using different cell-type-specific drivers. Depletion of p115 in the somatic cyst lineage and the hub caused no obvious defects, while depletion of p115 in germline cells resulted in complete germline cell loss (Figures S2C–S2H). Identical

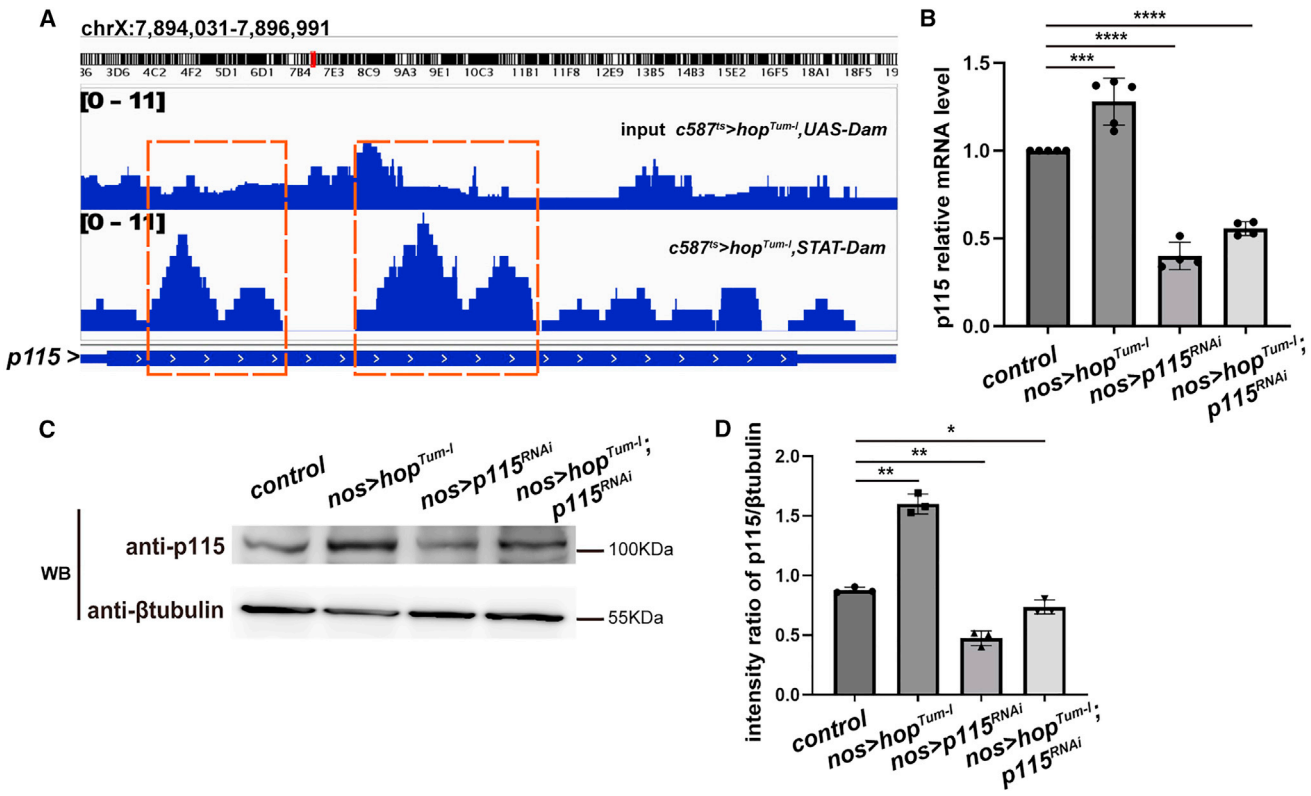

Figure 1. p115 is a putative downstream target of JAK/STAT signaling in *Drosophila* testis

(A) Dam-ID analysis for Stat92E reveals binding peaks of Stat92 E at the *p115* region (orange dashed boxes).

(B) qRT-PCR quantification of *p115* mRNA levels in testes with indicated genotypes. Mean ± SD is shown ($n \geq 4$). Two-tailed Student's t test was used. ***$p < 0.001$, ****$p < 0.0001$.

(C) Western blot analysis of p115 protein levels in the adult testes with indicated genotypes. β-Tubulin was used as blotting control.

(D) Quantification of p115 protein levels in testes with indicated genotypes by western blot analysis. Blot band intensity ratio of p115/β-tubulin shows similar trend with qRT-PCR in (B). Data are shown as mean ± SD (n = 3). Ordinary one-way ANOVA test was used. *$p < 0.05$, **$p < 0.01$.

defects were observed in testes depleting p115 in germline cells using additional RNAi constructs against *p115* (Figures S2I–S2K). These data indicate that p115 plays an essential role in germline cells but not somatic cyst cells and the hub.

Next, we determined the function of p115 in germline cells. We found that depletion of p115 in germline cells resulted in gradual loss of germline cells and enlarged hub, and eventually germline cells were totally lost and a giant hub was formed 8 days after eclosion (Figures 2A–2C, S2I–S2K, and S3A). To exclude the possibility of an off-target effect, we performed rescue experiments. Overexpression of p115 completely rescued the defects caused by induction of two different *p115* RNAi constructs (Figures S3A–S3D). We counted the number of GSCs at 0, 24, and 72 h after eclosion between control and *p115*-depleted testes (Figures 2D–2G). In control, each testis contained 6.750 ± 0.9 GSCs (n = 24) at 0 h, 6.381 ± 0.8 GSCs (n = 21) at 24 h, and 6.429 ± 0.6 GSCs (n = 21) at 72 h after eclosion, respectively. While *nos* > $p115^{RNAi}$ testis hosted fewer GSCs and the number of GSCs per testis gradually decreased from 5.727 ± 1.2 (n = 33) at 0 h, to 3.261 ± 2.1 (n = 23) at 24 h, and to 1.16 ± 1.2 (n = 26) at 72 h after eclosion (Figures 2D–2G). About 88% of *p115* knockdown testes contained less than two GSCs at 72 h after eclosion. These data suggest that p115 may play a role in GSC maintenance. The loss of GSCs may be caused by precocious GSC differentiation or cell death of GSCs. To discriminate these possibilities, we examined whether GSC loss observed in *p115*-depleted testis was caused by apoptotic cell death. However, no elevated apoptotic signal was observed in germline cells of *p115* knockdown testis (Figures S3E and S3F). Moreover, branched fusome was detected in p115-depleted germline cells attaching to the hub (Figure 2F). These data indicate that *p115*-deficient GSCs cannot maintain their stem cell fate and differentiate precociously but do not undergo apoptosis.

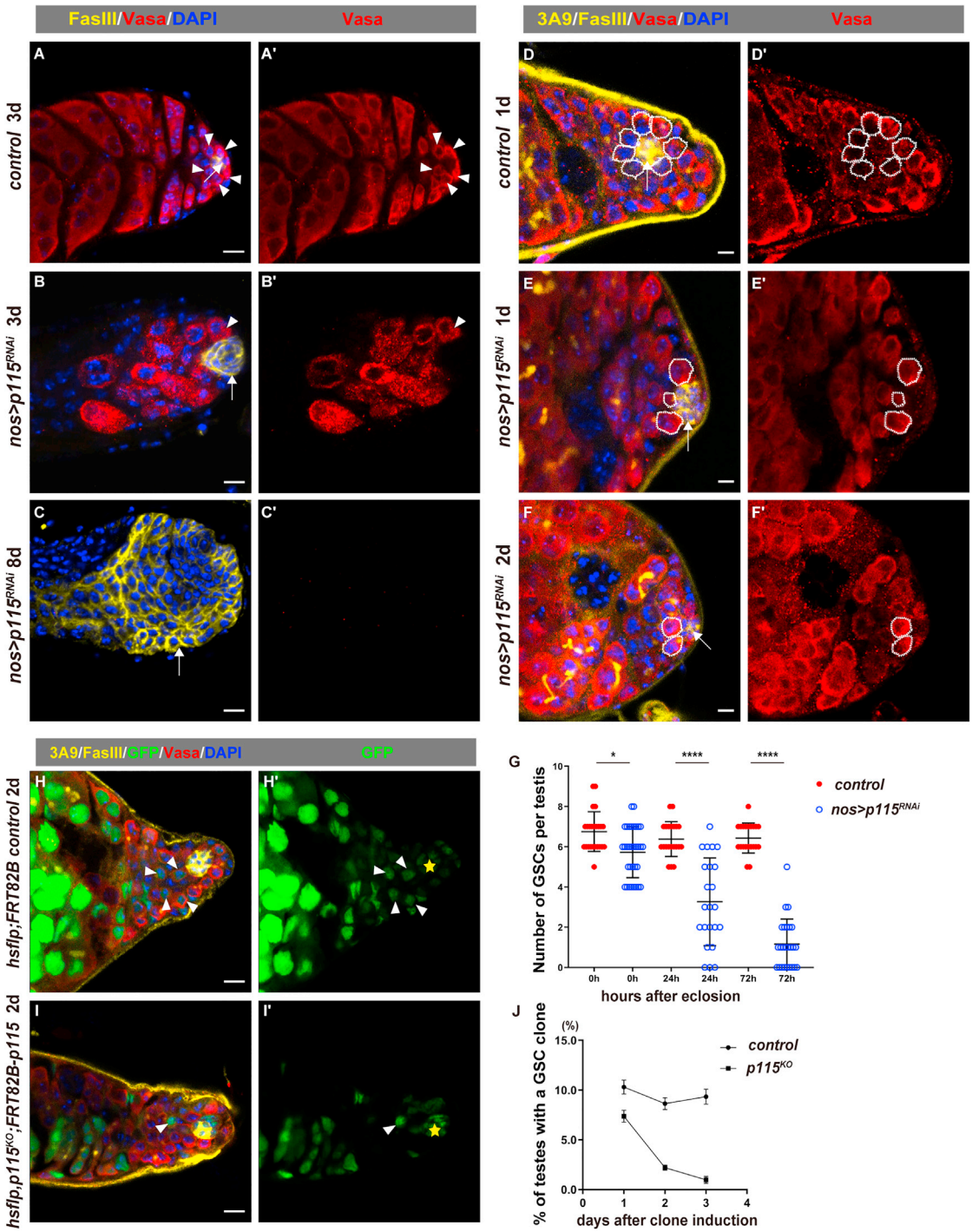

Figure 2. p115 is required for male GSC maintenance

(A–C) Representative confocal images of adult testis with indicated genotypes. The hub is indicated by white arrows and GSCs are indicated by white arrowheads.

(D–F) Representative confocal images of adult testis with indicated genotypes. The hub is indicated by arrows and GSCs are indicated by white dotted circles. 3A9 (yellow) is stained for the fusome.

(G) Quantification of the number of GSCs per testis in testes with indicated genotypes at different time points after eclosion. Mean ± SD is shown. Control testes: n = 24 at 0 h, n = 21 at 24 h, n = 21 at 72 h after eclosion. *nos > p115*^{RNAi} testes: n = 33 at 0 h, n = 23 at 24 h, n = 26 at 72 h after eclosion. Ordinary one-way ANOVA test was used. *p < 0.05, ****p < 0.0001.

(legend continued on next page)

To further confirm the conclusion that p115 maintains GSC fate, we generated *p115* knockout mutant by CRISPR-Cas9 (Figure S3G). As *p115* is on the X chromosome and homozygous $p115^{KO}$ mutants die at an early stage during development, it is impossible to directly generate $p115^{KO}$ mutant clones in testis using standard mosaic techniques. To circumvent this problem, we generated a transgenic fly carrying Flag-tagged p115 under its endogenous promoter (*p115P::p115-Flag*) to generate GSC clones of $p115^{KO}$ mutant using the mosaic technique (Figure S3H). Compared with control, $p115^{KO}$ mutant GSCs could not maintain their GSC fate and differentiated (Figures 2H and 2I). We further investigated GSC maintenance by examining the percentage of marked GSCs at different time points after clone induction (ACI). Compared with the marked control GSCs that remained in contact with the hub 3 days ACI, $p115^{KO}$ mutant GSCs were rapidly differentiated, and no marked $p115^{KO}$ mutant GSCs could be observed 3 days ACI (Figure 2J). Altogether, these data indicate that p115 is intrinsically required for male GSC maintenance.

GM130 and GRASP65 are dispensable for male GSC maintenance

Golgins (such as p115, GM130, and giantin) and the GRASP family of Golgi stacking proteins (e.g., GRASP65) have been shown to play critical roles in maintaining the structure and dynamic nature of the Golgi apparatus (Barr et al., 1997; Linstedt and Hauri, 1993; Nakamura et al., 1995; Radulescu et al., 2011; Shorter et al., 2002). Previous studies showed that p115 interacts with GM130, and GM130 interacts with GRASP65 to maintain the structure of the Golgi apparatus (Barr et al., 1997, 1998; Dirac-Svejstrup et al., 2000; Kondylis et al., 2001; Nakamura et al., 1995). We then examined whether GM130 and GRASP65 function together with p115 to maintain GSC fate in *Drosophila* testis. Interestingly, no obvious defects were observed upon depletion of either GM130 or GRASP65 in germline cells, indicating that, unlike p115, GM130 and GRASP65 are not required for male GSC maintenance (Figures S4A–S4E). In support of this notion, the number of male GSCs in homozygous *GM130* and *GRASP65* mutants was comparable with that of the wild type (Figures S4E–S4G). These data show that GM130 and GRASP65 are dispensable for male GSC maintenance and p115 maintains male GSC fate independent of GM130 and GRASP65.

Depletion of p115 affects the morphology of the ER and the Golgi apparatus

We used p115-specific antibody (Figure S1) and *p115P::p115-Flag* transgenic fly to examine the expression pattern and subcellular localization of p115. We found that p115 is mainly expressed in germline cells and is localized in cytoplasm in a punctate pattern by both p115 antibody and Flag staining (Figures S1A and S5A). The results of p115 antibody staining with the ER marker (KDEL-GFP) and Golgi resident protein (mannosidase II-GFP [Man II-GFP]) showed that p115 mainly localizes in the cytoplasm, the ER, and partially in the Golgi apparatus (Figures 3A and 3B). Consistently, germline-expressed Flag-tagged p115 puncta also co-localized with the ER and partially with the Golgi apparatus (Figures S5B and S5C). These results indicate that p115 is mainly localized in cytosol, but also in the ER and Golgi apparatus in germline cells, which is consistent with previous reports (Alvarez et al., 1999; Kondylis and Rabouille, 2003).

A previous study reported that p115 depletion in *Drosophila* S2 cells led to morphological changes in the Golgi stack morphology and the tER organization (Kondylis and Rabouille, 2003). We examined whether p115 depletion in germline cells affects the morphology of the ER and Golgi apparatus. We found that p115 depletion caused morphological changes of the ER and Golgi apparatus, from focused dots to dispersion (Figures 3C–3G). About 98% of control germline cells contained at least one KDEL-GFP (the ER marker) punctum, while about 60% of *p115*-depleted germline cells contained no KDEL-GFP puncta, with KDEL-GFP dispersed throughout the cytosol (Figures 3C–3E). Man II-GFP (the Golgi apparatus marker) forms puncta in about 97% of control germline cells; however, only about 64% of *p115*-depleted germline cells contained at least one Man II-GFP punctum (Figures 3E–3G). To further confirm this, we examined the morphology of the ER and Golgi apparatus by conventional transmission electron microscopy (TEM). We found the structure of ER in *p115*-depleted germline cells became inflated compared with that in control germline cells (Figures 3H and 3I). Meanwhile, compared with control germline cells, the Golgi apparatus formed clusters of vesicles and short tubules in *p115*-depleted germline cells (Figures 3H and 3I). Together, these results indicate that p115 is required for the organization of the ER and Golgi apparatus in male germline cells.

(H) Wild-type GSC clones (white arrowheads) (2 days ACI). The hub is indicated by yellow asterisks. GFP channel is shown separately.
(I) $p115^{KO}$ GSC clones fail to maintain GSC fate and differentiate to spermatogonia (white arrowheads) (2 days ACI).
(J) Percentage of the testes carrying a marked WT or $p115^{KO}$ mutant GSC clone over time (1–3 days ACI). Three replicates, $n \geq 42$. Vasa (red) is stained for germline cells, FasIII (yellow) is stained for the hub, 3A9 (yellow) is stained for the fusome and DAPI (blue) is stained for the nucleus. Scale bars, 5 and 10 μm in (A–C).

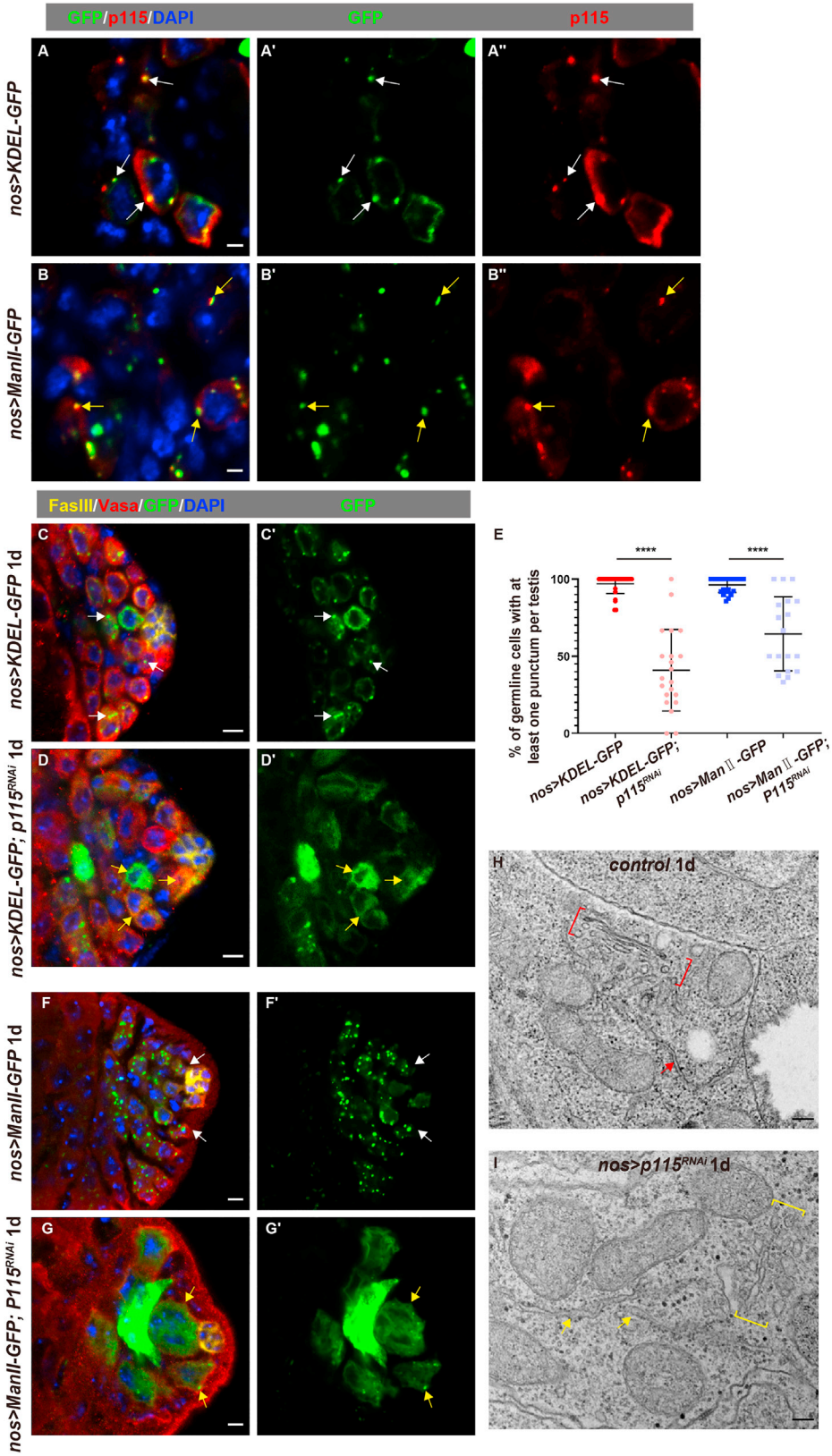

(legend on next page)

Depletion of p115 caused spindle orientation changes in male GSCs

A study in mammalian cells suggests a functional association of p115 with the structure and function of the late mitotic spindle as well as with resolution of the cytokinetic bridge (Radulescu et al., 2011). In addition, about 60% of *p115*-depleted *Drosophila* S2 cells exhibited abnormal and multipolar spindles with varied aberrant morphologies and misaligned chromosomes (Ibar and Glavic, 2017). We investigated whether knockdown of p115 in male GSCs resulted in any abnormalities in the structure and orientation of the mitotic spindles. We quantified metaphase spindle orientation in control and *nos* > $p115^{RNAi}$ GSCs by measuring the angle formed between the hub and the dividing spindles (Figures 4A and 4B). The metaphase division angles concentrated around 85° in control GSCs which are nearly perpendicular to the hub, whereas the division angles in *nos* > $p115^{RNAi}$ GSCs were randomly spread (Figure 4C). JAK/STAT signaling in GSCs regulates the orientation of their mitotic spindles perpendicular to the hub, which ensures that one stem cell daughter stays close to the hub and maintains stem cell identity while the other is displaced away from the hub and begins to differentiate (Deng and Lin, 1997; Yamashita et al., 2003). These data imply that the mis-orientation of the centrosomes in *p115*-depleted GSCs may be a consequence of aberrant JAK/STAT signaling, thereby *p115*-depleted GSCs cannot maintain stem cell identity and undergo differentiation.

The levels of pStat92E and Stat92E are diminished in *p115*-depleted male GSCs

Next, we explored whether JAK/STAT signaling is affected in the absence of p115. We examined the activation of JAK/STAT signaling in GSCs by pStat92E (pSTAT), a well-established readout of JAK/STAT signaling (Zhang et al., 2013). Interestingly, the levels of pStat92E in *p115*-depleted GSCs were dramatically reduced at less than 1 day after eclosion compared with those in the control GSCs (Figures 5A–5C). Furthermore, the western blotting results showed that the levels of pStat92E were significantly reduced in *p115*-depleted testis (Figure 5D). The diminished levels of pStat92E observed in *p115*-depleted GSCs may be due to significant reduction of JAK/STAT signaling or decreased levels of Stat92E protein. To discriminate these two possibilities, we examined the levels of Stat92E in GSCs using an endogenous *Stat92E-Flag-GFP* reporter. We found that the levels of endogenous Stat92E were greatly diminished in *p115*-depleted GSCs compared with those of control (Figures 5A–5C). These data suggest that p115 may regulate JAK/STAT signaling by affecting the protein levels of Stat92E to ensure proper spindle orientation in GSCs and maintain GSC fate. To further confirm this, we examined the levels of pStat92E and Stat92E in GSCs at different time points after eclosion. We observed that the levels of pStat92E in *p115*-depleted GSCs gradually and significantly decreased from 0 to 30 h after eclosion, accompanied by great reduction of GSC number, suggesting that GSCs are gradually lost due to differentiation (Figures 5E–5J). In support of this notion, we found that the protein levels of Stat92E were also gradually and significantly diminished in *p115*-depleted GSCs compared with those of the control (Figures 5K–5P). Altogether, these data show that p115 sustains the levels of Stat92E in GSCs to ensure JAK/STAT signaling activation for male GSC maintenance.

We further examined the levels of pStat92E in CySCs when *p115* was depleted or overexpressed. The results showed that both knockdown and overexpression of *p115* in GSCs did not significantly affect JAK/STAT signaling activity in CySCs (Figure S6). Moreover, overexpression of *p115* in GSCs did not significantly affect the levels of pStat92E in GSCs, indicating that p115 is

Figure 3. p115 depletion affects the morphology of the ER and Golgi apparatus

(A) p115 (red) localizes in the ER (by KDEL-GFP in green, white arrows). p115 and GFP channels are shown separately. Please note that the transgene is not equally expressed in germline cells when driven by *nosGal4* (the same as follows).

(B) p115 (red) localizes in the Golgi apparatus (by Man II-GFP in green, yellow arrows). p115 and GFP channels are shown separately.

(C and D) Depletion of p115 affects the morphology of the ER. The ER in control mainly appears as dots in cytoplasm (C) (white arrows) and becomes dispersed in *p115*-depleted cells (D) (yellow arrows). GFP channels are shown separately.

(E) Quantification of the percentage of germline cells with at least one KDEL-GFP or Man II-GFP punctum per testis in testes with indicated genotypes at 1 day after eclosion. Mean ± SD is shown. n = 27 for *nos* > *KDEL-GFP;* w^{RNAi} as control, n = 22 for *nos* > *KDEL-GFP;* $p115^{RNAi}$, n = 24 for *nos* > *Man II-GFP;* w^{RNAi} as control, and n = 18 for *nos* > *Man II-GFP;* $p115^{RNAi}$. Two-tailed Student's t test was used. ****p < 0.0001.

(F and G) Depletion of p115 affects the morphology of the Golgi apparatus. The Golgi apparatus in control testis appears as dots in cytoplasm (F) (white arrows) and becomes mainly dispersed in *p115*-depleted testis (G) (yellow arrows). GFP channels are shown separately.

(H and I) TEM images from germline cells in the control (H) or *p115*-depleted testis (I). The ER is indicated with arrows. The red arrow indicates the ER in control germline cells and the yellow arrows indicate the ER in *p115*-depleted germline cells. The Golgi areas are marked between brackets. In control germline cells, the Golgi stacks can be seen between red brackets. While clusters of vesicles and short tubules are observed in the Golgi area in *p115*-depleted germline cells (between yellow brackets). Vasa (red) is stained for germline cells, FasIII (yellow) is stained for the hub, and DAPI (blue) is stained for the nucleus. Scale bars, 5 μm, 2 μm in (A and B), and 200 nm in (H and I).

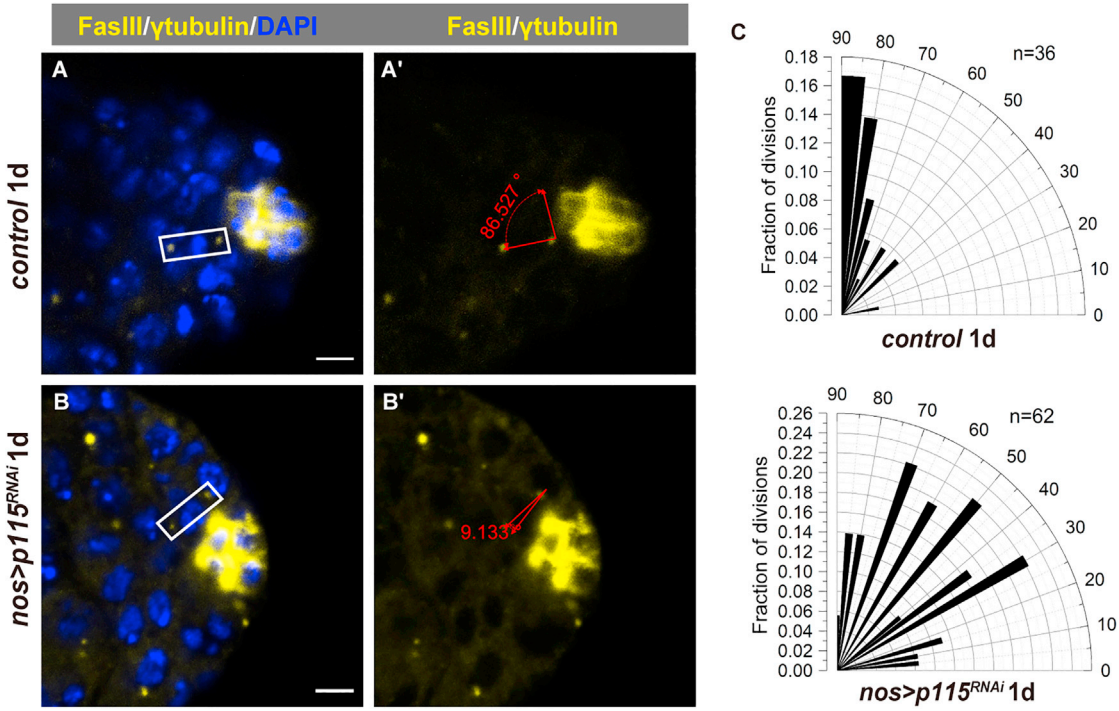

Figure 4. p115 depletion affects spindle orientation

(A and B) Representative images of division angles of the mitotic spindles (by γ-tubulin in yellow) in control (A) and *nos > p115*^{RNAi} GSCs (B). (C) Radial histogram quantification of division angles in control (n = 36) and p115 depleted (n = 62) metaphase GSCs at 1 day after eclosion. γ-Tubulin (yellow) is stained for the centrosome and DAPI (blue) is stained for the nucleus. Scale bars, 5 μm.

necessary but not sufficient for JAK/STAT signaling activation (Figures S6C and S6D).

p115 associates with and stabilizes Stat92E

The abovementioned data show that p115 maintains male GSC fate by regulating the levels of Stat92E. We then investigated the underlying mechanism of p115 in male GSC maintenance. Interestingly, we found that transiently expressed p115 partially co-localized with endogenous Stat92E in GSCs, suggesting that they may associate with each other in GSCs (Figure 6A). Consistently, transiently expressed p115 also partially co-localized with transiently expressed Stat92E in germline cells (Figure 6B). We then performed co-immunoprecipitation (coIP) experiments to examine whether they are associated *in vivo*. The coIP results showed that p115 interacts with Stat92E (Figure 6C). Collectively, our data demonstrate that p115 associates with and stabilizes Stat92E to maintain male GSC fate. To functionally determine whether diminished Stat92E protein levels are responsible for the defects associated with p115 depletion, we asked whether GSC loss observed in the absence of p115 could be rescued by restoration of Stat92E proteins. Ectopic expression of wild type Stat92E completely restored the GSC loss defects observed in *nos > p115*^{RNAi} testes (Figures 6D–6H). These results show that p115 maintains male GSC fate by associating with and stabilizing Stat92E. Taken together, these data indicate that activation of JAK/STAT signaling in GSCs promotes the expression of p115, which in turn associates with and stabilizes Stat92E protein to sustain JAK/STAT signaling duration, forming a feedforward loop to maintain male GSC fate.

DISSCUSION

The balance of GSC self-renewal and differentiation in *Drosophila* testis is controlled by many signals. The JAK/STAT signaling is the most important pathway to regulate GSC maintenance (Kiger et al., 2001; Tulina and Matunis, 2001; Yamashita et al., 2003). However, how GSC maintenance is regulated by JAK/STAT signaling and its downstream target regulators are not fully understood. Here, we identify p115, a tER/*cis*-Golgi golgin protein, as a putative downstream target of JAK/STAT signaling and p115 in turn sustains JAK/STAT signaling activation. Loss of *p115* in GSCs reduced the protein levels of Stat92E and thus pStat92E, resulting in GSC loss. The biochemical and genetic data indicate that

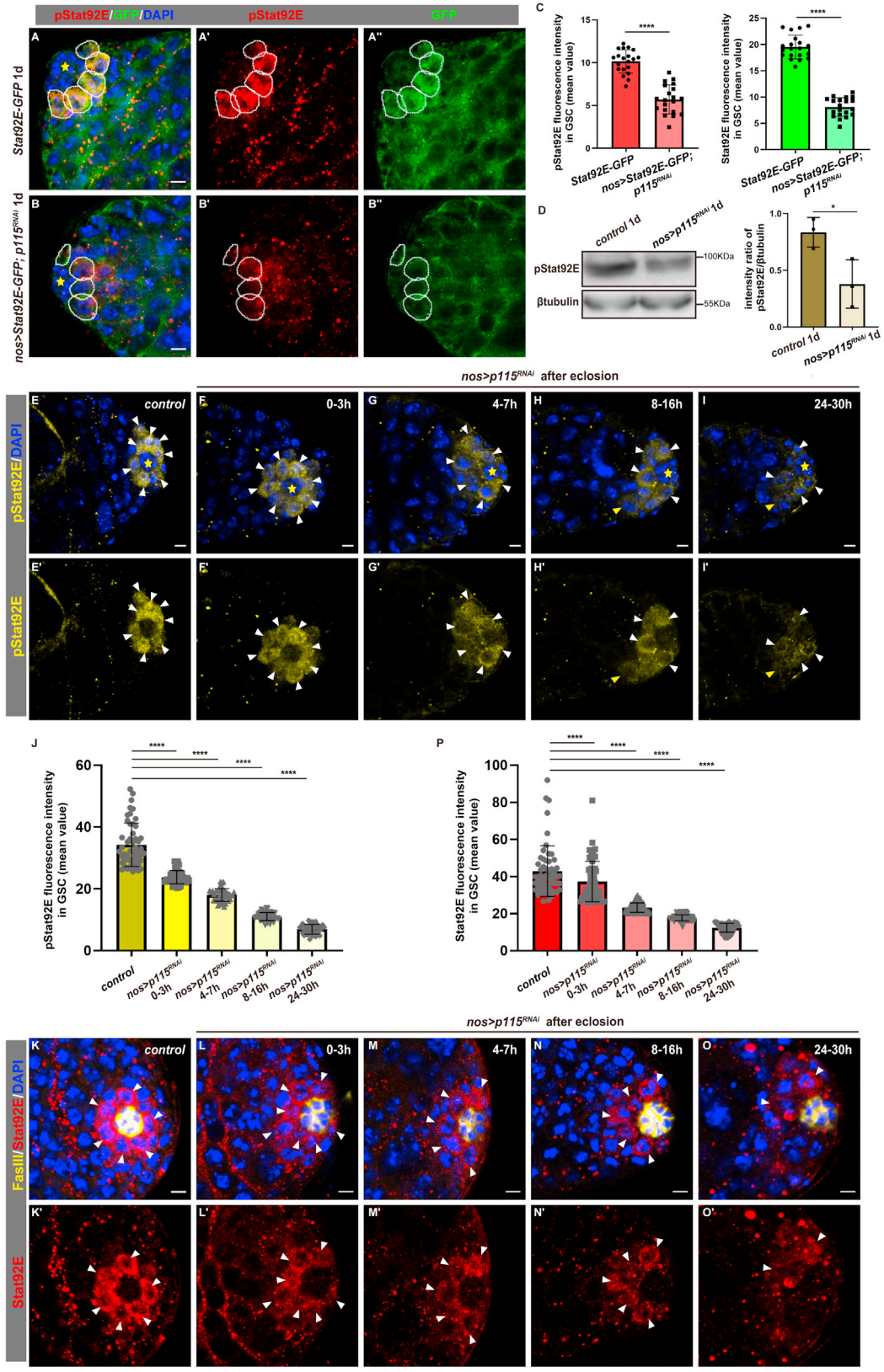

(legend on next page)

p115 associates with and stabilizes Stat92E to maintain male GSC identity.

Drosophila p115 protein shares high level of homology with its mammalian counterpart. Depletion of p115 in mammalian cells causes fragmentation of the Golgi ribbon and the formation of Golgi mini-stacks with delayed protein transport (Alvarez et al., 2001; Puthenveedu and Linstedt, 2001; Sohda et al., 2005). Depletion of *Drosophila* p115 in S2 cells led to a quantitative breakdown of Golgi stacks and strongly affected the general organization of the tER sites without affecting the intracellular transport (Kondylis and Rabouille, 2003). Our data show that knockdown of p115 in GSCs affects the morphology of the ER and Golgi apparatus, which is consistent with previous studies (Figure 3) (Kondylis et al., 2001; Kondylis and Rabouille, 2003). Meanwhile, golgins (GM130, giantin, and p115) and GRASP proteins (GRASP65 and GRASP55) play important roles in maintaining the structure of the Golgi apparatus (Barr et al., 1997; Barroso et al., 1995; Linstedt and Hauri, 1993; Nakamura et al., 1995; Shorter et al., 1999). Interestingly, our results show that GM130 (golgins) and GRASP65 (GRASP) are dispensable for male GSC maintenance, suggesting that p115 functions in a golgin- and GRASP-independent manner to maintain male GSC identity. *p115*-depleted mammalian cells (~80%) exhibited abnormal, multipolar spindles with a range of aberrant morphologies and misaligned chromosomes, which did not result in mitotic arrest and cell death (Radulescu et al., 2011). p115 function in the maintenance of the mitotic spindle is likely to be dependent on p115-γ-tubulin association and involved in the maintenance of centrosome integrity during mitosis and Golgi structure during cytokinesis completion (Radulescu et al., 2011). Consistent with results from mammalian cells, *p115*-depleted *Drosophila* S2 cells (~60%) exhibited abnormal, multipolar spindles with a range of aberrant morphologies and misaligned chromosomes (Ibar and Glavic, 2017). In our study, knockdown of p115 in GSCs did not cause obvious abnormalities in the structure of the mitotic spindles but caused high frequency of spindle mis-orientation. Male GSCs divide asymmetrically by orienting their mitotic spindles perpendicular to the hub-GSC interface (Yamashita et al., 2003). Misorienting the mitotic spindles perpendicular to the hub-GSC interface may predict GSC daughter cells' different cell fate, both by germ stem cells to self-renew or by GBs to initiate differentiation. JAK/STAT signaling in GSCs regulates the orientation of their mitotic spindles perpendicular to the hub to ensure GSC self-renewal and differentiation (Deng and Lin, 1997; Yamashita et al., 2003). Spindle mis-orientation in *p115*-depleted GSCs may be a consequence of defective JAK/STAT signaling in the absence of p115 and/or defective p115-γ-tubulin association, thereby leading to male GSC loss.

To maintain tissue homeostasis, organisms develop multiple regulatory mechanisms to control the duration and strength of signaling activation. The JAK/STAT pathway plays a critical role in maintaining the stem cell identity of both GSCs and CySCs (Kiger et al., 2001; Tulina and Matunis, 2001). Socs36E, a conserved transcriptional target of JAK/STAT signaling, negatively regulates the JAK/STAT signaling via distinct mechanisms to control the duration and strength of JAK/STAT signaling in both stem cell populations (Arbouzova and Zeidler, 2006; Callus and Mathey-Prevot, 2002; Rawlings et al., 2004). Here, we show that p115 is a putative downstream target of JAK/STAT signaling. Importantly, p115 sustains JAK/STAT signaling by associating with and stabilizing Stat92E (STAT). Given that STAT is a cytosol and nuclear protein and p115 is generally believed to be an ER/Golgi protein, how could

Figure 5. The levels of pStat92E and Stat92E are diminished in *p115*-depleted GSCs

(A) The levels of pStat92E (red) and Stat92E (green, by Stat92E-Flag-GFP) in control GSCs. GSCs are indicated by white dotted circles. The hub is indicated by asterisks. pStat92E and Stat92E channels are shown separately.

(B) The levels of pStat92E (red) and Stat92E (green, by Stat92E-Flag-GFP) are greatly diminished in *nos* > $p115^{RNAi}$ GSCs.

(C) Quantification of the average fluorescent intensity of pStat92E and Stat92E in control and *nos* > $p115^{RNAi}$ GSCs. Mean ± SD is shown (n = 20). Two-tailed Student's t test was used. ****p < 0.0001.

(D) Western blot analysis and quantification of the levels of pStat92E protein in adult testes with indicated genotypes. β-Tubulin was used as blotting control. Data are shown as mean ± SD (n = 3). Two-tailed Student's t test was used. *p < 0.05.

(E–I) Representative confocal images of pStat92E (yellow) staining in adult testes of control and *nos* > $p115^{RNAi}$ at different time points after eclosion. The levels of pStat92E gradually reduced over time in *p115*-depleted GSCs (white arrowheads). The GBs with high pStat92E levels are indicated by yellow arrowheads. The hub is indicated by yellow asterisks. pStat92E channels are shown separately.

(J) Quantification of the average fluorescent intensity of pStat92E in testes with indicated genotypes at different time points after eclosion. Mean ± SD is shown (n ≥ 45). Ordinary one-way ANOVA test was used. ****p < 0.0001.

(K–O) Representative confocal images of Stat92E staining (red) in adult testes of control and *nos* > $p115^{RNAi}$ at different time points after eclosion. The levels of Stat92E gradually reduced over time in *p115*-depleted GSCs (white arrowheads). The hub is stained by FasIII in yellow. Stat92E channels are shown separately.

(P) Quantification of the average fluorescent intensity of Stat92E in testes with indicated genotypes ate different time points after eclosion. Mean ± SD is shown (n ≥ 55). Ordinary one-way ANOVA test was used. ****p < 0.0001. Scale bars, 5 μm.

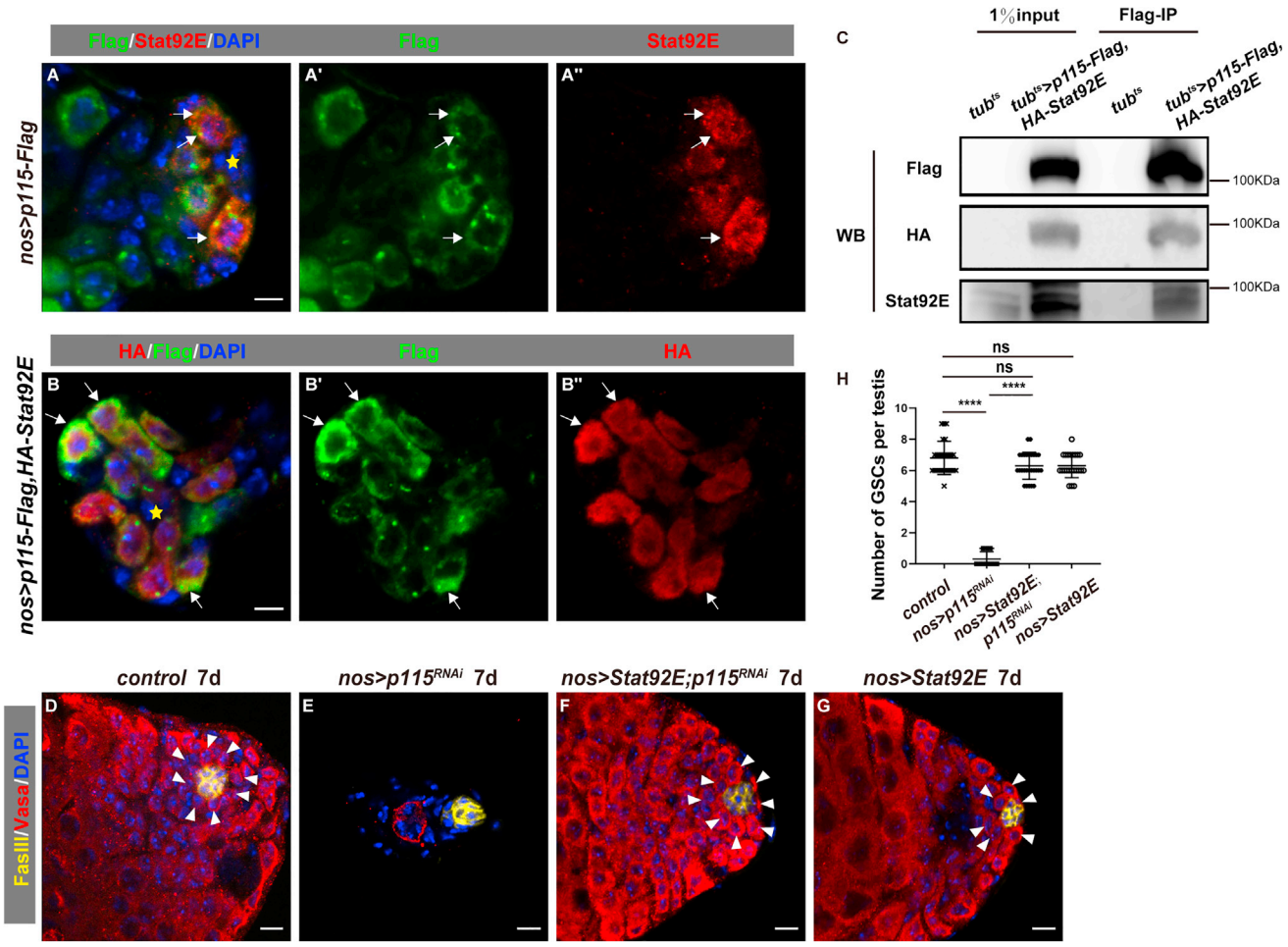

Figure 6. Biochemical and genetics interactions between p115 and Stat92E

(A) Endogenous Stat92E (red) and transiently expressed p115-Flag (green, by Flag) partially co-localized in GSCs (white arrows). Asterisk marks the hub. Flag and Stat92E channels are shown separately.

(B) Transiently expressed Stat92E (red, by HA) and transiently expressed p115 (green, by Flag) partially co-localized in germline cells (white arrows). Flag and HA channels are shown separately.

(C) Physical interaction between p115 and Stat92E. Lysate from tub^{ts} flies was used as negative control.

(D–G) The phenotype of *p115* knockdown (E) can be fully rescued by overexpression of *Stat92E* (F) compared with control (D). And overexpression of *Stat92E* has no obvious phenotype (G) compared with control (D). White arrowheads indicate GSCs. Vasa is stained for germline cells and FasIII is stained for the hub.

(H) Quantification of the number of GSCs per testis in testes with indicated genotypes. Mean ± SD is shown. n = 26 for *nos* > w^{RNAi} as control, n = 25 for *nos* > $p115^{RNAi}$, n = 27 for *nos* > *Stat92E*, $p115^{RNAi}$, and n = 23 for *nos* > *Stat92E*. Ordinary one-way ANOVA test was used, ns, not significant, ****p < 0.0001. DAPI is stained in blue for the nucleus. Scale bars, 5 μm in (A and B) and 10 μm (D–G).

p115 associate with and stabilize STAT to maintain stem cell fate? In mammalian cells, p115 has been shown to have at least three roles. First, p115 is a highly conserved, vesicle-tethering protein, required for Golgi organization and ER-Golgi transport (Shorter and Warren, 2002). Second, p115 interacts with macrophage migration inhibitory factor (MIF) in the cytoplasm and promotes MIF release from the perinuclear ring to the plasma membrane and then out of the cell in conjunction with MIF by an unconventional route for protein export (Li et al., 2013; Merk et al., 2009). Third, p115 associates with long-chain acyl-CoA synthetase 4 (ACSL4) in the presence of AA, ACSL4's substrate, and is involved in the degradation of ACSL4 through the ubiquitin-proteasomal pathway (Sen et al., 2020). Given the significant homology between p115 and its mammalian counterpart, p115 could have an equivalent role in stabilizing ER and Golgi structure or proteins, which is supported by the observation that the morphology of the ER and Golgi apparatus is affected in the absence of p115 (Figure 3). Here, we find that p115

localizes mainly in cytoplasm, and the ER/Golgi apparatus in male germline cells associates with and stabilizes STAT. We speculate that the cytosolic p115 interacts with and stabilizes STAT which is independent of its roles in the ER and Golgi apparatus, while the ER/Golgi-localized p115 is responsible for the morphology of the ER and Golgi apparatus. Although the morphology of the ER and Golgi apparatus and spindle orientation are affected upon p115 depletion, as JAK/STAT signaling is pivotal for male GSC maintenance, thus the main effect of p115 depletion is defective JAK/STAT signaling due to de-stabilized STAT.

Therefore, JAK/STAT and p115 form a feedforward loop in GSCs to ensure proper JAK/STAT activity required for male GSC maintenance. This feedforward loop is further supported by the observation that excessive GSCs resulting from ectopic expression of constitutively active $Hop^{Tum\text{-}l}$ were effectively suppressed by p115 depletion, as Stat92E became unstable in the absence of p115, and thus be the limiting factor for JAK/STAT signaling activation and male GSC maintenance in p115-depleted testes. Meanwhile, overexpression of p115, which is similar to Stat92E overexpression, did not cause excessive JAK/STAT signaling activation and increased number of GSCs, indicating that p115 is necessary but not sufficient for JAK/STAT signaling activation. Given that both JAK/STAT signaling and p115 are well conserved, our work provides new insights into the regulatory mechanism of how stem cell maintenance is properly controlled by JAK/STAT signaling.

EXPERIMENTAL PROCEDURES

Resource availability

Corresponding author

Further information and requests for resources and reagents should be directed to and will be fulfilled by the corresponding author, Zhouhua Li (zhli@cnu.edu.cn).

Materials availability

All unique and stable reagents generated in this study of which sufficient quantities exists are available from the corresponding author with a complete Materials Transfer Agreement.

Data and code availability

The Dam-ID data have been deposited under NCBI GEO accession no. GSE226582.

Fly lines and cultures

Flies were maintained on standard medium at 25°C. Crosses were raised at 18°C in humidity-controlled incubators, or as otherwise noted. Information for alleles and transgenes used in this study can be found either in FlyBase or as noted.

Immunostainings and fluorescence microscopy

Standard immunostaining of intestines was followed as described previously (Zhao et al., 2021). The following primary antibodies were used: rabbit anti-Zfh-1 (1:50,000; Xu et al., 2018), rabbit anti-Vasa (d-260, 1:200, Santa Cruz, cat no. sc-30210), rabbit anti-Vasa (1:2,000; Zhao et al., 2022), mouse anti-α-spectrin (3A9, 1:50, developed by D. Branton and R. Dubreuil, Developmental Studies Hybridoma Bank [DSHB]), mouse anti-FasIII (7G10, 1:100, developed by C.S. Goodman, DSHB), rabbit anti-GFP (1:1,000, Abcam), mouse anti-γ-tubulin (1:1,000, Abbkine), guinea pig anti-Stat92E (1:1,000, a generous gift from Dr. Yu Cai), mouse anti-pStat92E (1:2,000, Abmart, China; Zhang et al., 2013), rabbit anti-β-galactosidase (lacZ, 1:5,000, Cappel, cat. no. 55978), and mouse anti-Flag (1:2,000, Sigma-Aldrich). All images were captured using a Zeiss LSM780 inverted confocal microscope and were processed in Adobe Photoshop and Illustrator.

SUPPLEMENTAL INFORMATION

Supplemental information can be found online at https://doi.org/10.1016/j.stemcr.2023.08.007.

AUTHOR CONTRIBUTIONS

Conceptualization, Z.H.L. and R.Y.K.; methodology, R.Y.K.; validation, Z.H.L. and R.Y.K.; data curation, Z.H.L., R.Y.K., and F.L.L.; formal analysis, R.Y.K. and J.L.; investigation: R.Y.K., J.L., Y.K.M., H.Z., H.F.Z., and M.F.M.; writing, Z.H.L. and R.Y.K.; project administration, Z.H.L.; funding acquisition, Z.H.L.; supervision, Z.H.L.

ACKNOWLEDGMENTS

We are grateful to Drs. Andrea Brand, Yu Cai, Erika A. Bach, Dahua Chen, Zhou Wei, Gyeong-Hun Baeg, Jianquan Ni, DSHB, Bloomington *Drosophila* Stock Center, VDRC, NIG-FLY stock center, and TRiP for reagents and stocks. We also thank Jun Chen from Rongwen Xi lab, and Peng Zhang and Yongqiang Wang for suggestions and help on Dam-ID. We are grateful to Yanfei Hu and Cell Biology Facility in Tsinghua University for TEM. This work is supported by grants from the National Natural Science Foundation of China (nos. 92054109, 31972893, and 31471384) and Beijing Municipal Commission of Education (no. KZ201910028040).

CONFLICT OF INTERESTS

The authors declare no competing interests.

Received: March 7, 2023
Revised: August 10, 2023
Accepted: August 11, 2023
Published: September 7, 2023

REFERENCES

Allan, B.B., Moyer, B.D., and Balch, W.E. (2000). Rab1 recruitment of p115 into a cis-SNARE complex: programming budding COPII vesicles for fusion. Science *289*, 444–448.

Alvarez, C., Fujita, H., Hubbard, A., and Sztul, E. (1999). ER to Golgi transport: Requirement for p115 at a pre-Golgi VTC stage. J. Cell Biol. *147*, 1205–1222.

Alvarez, C., Garcia-Mata, R., Hauri, H.P., and Sztul, E. (2001). The p115-interactive proteins GM130 and giantin participate in endoplasmic reticulum-Golgi traffic. J. Biol. Chem. *276*, 2693–2700.

Arbouzova, N.I., and Zeidler, M.P. (2006). JAK/STAT signalling in Drosophila: insights into conserved regulatory and cellular functions. Development *133*, 2605–2616.

Barlowe, C., Orci, L., Yeung, T., Hosobuchi, M., Hamamoto, S., Salama, N., Rexach, M.F., Ravazzola, M., Amherdt, M., and Schekman, R. (1994). COPII: a membrane coat formed by Sec proteins that drive vesicle budding from the endoplasmic reticulum. Cell *77*, 895–907.

Barr, F.A., Nakamura, N., and Warren, G. (1998). Mapping the interaction between GRASP65 and GM130, components of a protein complex involved in the stacking of Golgi cisternae. EMBO J. *17*, 3258–3268.

Barr, F.A., Puype, M., Vandekerckhove, J., and Warren, G. (1997). GRASP65, a protein involved in the stacking of Golgi cisternae. Cell *91*, 253–262.

Barroso, M., Nelson, D.S., and Sztul, E. (1995). Transcytosis-associated protein (TAP)/p115 is a general fusion factor required for binding of vesicles to acceptor membranes. Proc. Natl. Acad. Sci. USA *92*, 527–531.

Binari, R., and Perrimon, N. (1994). Stripe-specific regulation of pair-rule genes by hopscotch, a putative Jak family tyrosine kinase in Drosophila. Genes Dev. *8*, 300–312.

Blanpain, C., and Fuchs, E. (2014). Stem cell plasticity. Plasticity of epithelial stem cells in tissue regeneration. Science *344*, 1242281.

Callus, B.A., and Mathey-Prevot, B. (2002). SOCS36E, a novel Drosophila SOCS protein, suppresses JAK/STAT and EGF-R signalling in the imaginal wing disc. Oncogene *21*, 4812–4821.

Chandel, N.S., Jasper, H., Ho, T.T., and Passegué, E. (2016). Metabolic regulation of stem cell function in tissue homeostasis and organismal ageing. Nat. Cell Biol. *18*, 823–832.

Corwin, H.O., and Hanratty, W.P. (1976). Characterization of a Unique Lethal Tumorous Mutation in Drosophila. Mol. Gen. Genet. *144*, 345–347.

Davies, E.L., and Fuller, M.T. (2008). Regulation of self-renewal and differentiation in adult stem cell lineages: lessons from the Drosophila male germ line. Cold Spring Harbor Symp. Quant. Biol. *73*, 137–145.

de Cuevas, M., and Matunis, E.L. (2011). The stem cell niche: lessons from the Drosophila testis. Development *138*, 2861–2869.

Decotto, E., and Spradling, A.C. (2005). The Drosophila ovarian and testis stem cell niches: similar somatic stem cells and signals. Dev. Cell *9*, 501–510.

Deng, W., and Lin, H. (1997). Spectrosomes and fusomes anchor mitotic spindles during asymmetric germ cell divisions and facilitate the formation of a polarized microtubule array for oocyte specification in Drosophila. Dev. Biol. *189*, 79–94.

Dirac-Svejstrup, A.B., Shorter, J., Waters, M.G., and Warren, G. (2000). Phosphorylation of the vesicle-tethering protein p115 by a casein kinase II-like enzyme is required for Golgi reassembly from isolated mitotic fragments. J. Cell Biol. *150*, 475–488.

Flaherty, M.S., Salis, P., Evans, C.J., Ekas, L.A., Marouf, A., Zavadil, J., Banerjee, U., and Bach, E.A. (2010). chinmo is a functional effector of the JAK/STAT pathway that regulates eye development, tumor formation, and stem cell self-renewal in Drosophila. Dev. Cell *18*, 556–568.

Fuller, M.T., and Spradling, A.C. (2007). Male and female Drosophila germline stem cells: two versions of immortality. Science *316*, 402–404.

Gutierrez-Triana, J.A., Mateo, J.L., Ibberson, D., Ryu, S., and Wittbrodt, J. (2016). iDamIDseq and iDEAR: an improved method and computational pipeline to profile chromatin-binding proteins. Development *143*, 4272–4278.

Hanratty, W.P., and Dearolf, C.R. (1993). The Drosophila-Tumorous-Lethal Hematopoietic Oncogene Is a Dominant Mutation in the Hopscotch Locus. Mol. Gen. Genet. *238*, 33–37.

Hardy, R.W., Tokuyasu, K.T., Lindsley, D.L., and Garavito, M. (1979). The germinal proliferation center in the testis of Drosophila melanogaster. J. Ultrastruct. Res. *69*, 180–190.

Harrison, D.A., Binari, R., Nahreini, T.S., Gilman, M., and Perrimon, N. (1995). Activation of a Drosophila-Janus-Kinase (Jak) Causes Hematopoietic Neoplasia and Developmental Defects. EMBO J. *14*, 2857–2865.

Ibar, C., and Glavic, Á. (2017). Drosophila p115 is required for Cdk1 activation and G2/M cell cycle transition. Mech. Dev. *144*, 191–200.

Issigonis, M., Tulina, N., de Cuevas, M., Brawley, C., Sandler, L., and Matunis, E. (2009). JAK-STAT signal inhibition regulates competition in the Drosophila testis stem cell niche. Science *326*, 153–156.

Kiger, A.A., Jones, D.L., Schulz, C., Rogers, M.B., and Fuller, M.T. (2001). Stem cell self-renewal specified by JAK-STAT activation in response to a support cell cue. Science *294*, 2542–2545.

Kondylis, V., Goulding, S.E., Dunne, J.C., and Rabouille, C. (2001). Biogenesis of Golgi stacks in imaginal discs of Drosophila melanogaster. Mol. Biol. Cell *12*, 2308–2327.

Kondylis, V., and Rabouille, C. (2003). A novel role for dp115 in the organization of tER sites in Drosophila. J. Cell Biol. *162*, 185–198.

Leatherman, J.L., and Dinardo, S. (2008). Zfh-1 controls somatic stem cell self-renewal in the Drosophila testis and nonautonomously influences germline stem cell self-renewal. Cell Stem Cell *3*, 44–54.

Levine, T.P., Rabouille, C., Kieckbusch, R.H., and Warren, G. (1996). Binding of the vesicle docking protein p115 to Golgi membranes is inhibited under mitotic conditions. J. Biol. Chem. *271*, 17304–17311.

Li, L., and Xie, T. (2005). Stem cell niche: structure and function. Annu. Rev. Cell Dev. Biol. *21*, 605–631.

Li, X.J., Luo, Y., and Yi, Y.F. (2013). P115 promotes growth of gastric cancer through interaction with macrophage migration inhibitory factor. World J. Gastroenterol. *19*, 8619–8629.

Linstedt, A.D., and Hauri, H.P. (1993). Giantin, a novel conserved Golgi membrane protein containing a cytoplasmic domain of at least 350 kDa. Mol. Biol. Cell *4*, 679–693.

Merk, M., Baugh, J., Zierow, S., Leng, L., Pal, U., Lee, S.J., Ebert, A.D., Mizue, Y., Trent, J.O., Mitchell, R., et al. (2009). The Golgi-Associated Protein p115 Mediates the Secretion of Macrophage Migration Inhibitory Factor. J. Immunol. *182*, 6896–6906.

Morrison, S.J., and Spradling, A.C. (2008). Stem cells and niches: mechanisms that promote stem cell maintenance throughout life. Cell *132*, 598–611.

Nakamura, N., Rabouille, C., Watson, R., Nilsson, T., Hui, N., Slusarewicz, P., Kreis, T.E., and Warren, G. (1995). Characterization of a cis-Golgi matrix protein, GM130. J. Cell Biol. *131*, 1715–1726.

Nelson, D.S., Alvarez, C., Gao, Y.S., García-Mata, R., Fialkowski, E., and Sztul, E. (1998). The membrane transport factor TAP/p115 cycles between the Golgi and earlier secretory compartments and contains distinct domains required for its localization and function. J. Cell Biol. *143*, 319–331.

Orci, L., Ravazzola, M., Meda, P., Holcomb, C., Moore, H.P., Hicke, L., and Schekman, R. (1991). Mammalian Sec23p homologue is restricted to the endoplasmic reticulum transitional cytoplasm. Proc. Natl. Acad. Sci. USA *88*, 8611–8615.

Puthenveedu, M.A., and Linstedt, A.D. (2001). Evidence that Golgi structure depends on a p115 activity that is independent of the vesicle tether components giantin and GM130. J. Cell Biol. *155*, 227–238.

Radulescu, A.E., Mukherjee, S., and Shields, D. (2011). The Golgi protein p115 associates with gamma-tubulin and plays a role in Golgi structure and mitosis progression. J. Biol. Chem. *286*, 21915–21926.

Rawlings, J.S., Rennebeck, G., Harrison, S.M.W., Xi, R., and Harrison, D.A. (2004). Two Drosophila suppressors of cytokine signaling (SOCS) differentially regulate JAK and EGFR pathway activities. BMC Cell Biol. *5*, 38.

Sen, P., Kan, C.F.K., Singh, A.B., Rius, M., Kraemer, F.B., Sztul, E., and Liu, J. (2020). Identification of p115 as a novel ACSL4 interacting protein and its role in regulating ACSL4 degradation. J. Proteonomics *229*, 103926.

Shorter, J., Beard, M.B., Seemann, J., Dirac-Svejstrup, A.B., and Warren, G. (2002). Sequential tethering of Golgins and catalysis of SNAREpin assembly by the vesicle-tethering protein p115. J. Cell Biol. *157*, 45–62.

Shorter, J., and Warren, G. (2002). Golgi architecture and inheritance. Annu. Rev. Cell Dev. Biol. *18*, 379–420.

Shorter, J., Watson, R., Giannakou, M.E., Clarke, M., Warren, G., and Barr, F.A. (1999). GRASP55, a second mammalian GRASP protein involved in the stacking of Golgi cisternae in a cell-free system. EMBO J. *18*, 4949–4960.

Sohda, M., Misumi, Y., Yoshimura, S.i., Nakamura, N., Fusano, T., Sakisaka, S., Ogata, S., Fujimoto, J., Kiyokawa, N., and Ikehara, Y. (2005). Depletion of vesicle-tethering factor p115 causes mini-stacked Golgi fragments with delayed protein transport. Biochem. Biophys. Res. Commun. *338*, 1268–1274.

Southall, T.D., and Brand, A.H. (2009). Neural stem cell transcriptional networks highlight genes essential for nervous system development. EMBO J. *28*, 3799–3807.

Spradling, A.C., Nystul, T., Lighthouse, D., Morris, L., Fox, D., Cox, R., Tootle, T., Frederick, R., and Skora, A. (2008). Stem cells and their niches: integrated units that maintain Drosophila tissues. Cold Spring Harbor Symp. Quant. Biol. *73*, 49–57.

Tulina, N., and Matunis, E. (2001). Control of stem cell self-renewal in Drosophila spermatogenesis by JAK-STAT signaling. Science *294*, 2546–2549.

van Steensel, B., and Henikoff, S. (2000). Identification of *in vivo* DNA targets of chromatin proteins using tethered dam methyltransferase. Nat. Biotechnol. *18*, 424–428.

Waters, M.G., Clary, D.O., and Rothman, J.E. (1992). A novel 115-kD peripheral membrane protein is required for intercisternal transport in the Golgi stack. J. Cell Biol. *118*, 1015–1026.

White-Cooper, H., Leroy, D., MacQueen, A., and Fuller, M.T. (2000). Transcription of meiotic cell cycle and terminal differentiation genes depends on a conserved chromatin associated protein, whose nuclear localisation is regulated. Development *127*, 5463–5473.

Wilson, P.G. (2005). Centrosome inheritance in the male germ line of Drosophila requires hu-li tai-shao function. Cell Biol. Int. *29*, 360–369.

Xu, R., Li, J., Zhao, H., Kong, R., Wei, M., Shi, L., Bai, G., and Li, Z. (2018). Self-restrained regulation of stem cell niche activity by niche components in the Drosophila testis. Dev. Biol. *439*, 42–51.

Yamashita, Y.M., Jones, D.L., and Fuller, M.T. (2003). Orientation of asymmetric stem cell division by the APC tumor suppressor and centrosome. Science *301*, 1547–1550.

Yan, R., Small, S., Desplan, C., Dearolf, C.R., and Darnell, J.E., Jr. (1996). Identification of a Stat gene that functions in Drosophila development. Cell *84*, 421–430.

Zhang, Y., You, J., Ren, W., and Lin, X. (2013). *Drosophila* glypicans Dally and Dally-like are essential regulators for JAK/STAT signaling and Unpaired distribution in eye development. Dev. Biol. *375*, 23–32.

Zhao, H., Li, Z., Kong, R., Shi, L., Ma, R., Ren, X., and Li, Z. (2022). Novel Intrinsic Factor Yun Maintains Female Germline Stem Cell Fate through Thickveins. Stem Cell Rep. *17*, 1914–1923.

Zhao, H., Shi, L., Kong, R., Li, Z., Liu, F., Zhao, H., and Li, Z. (2021). Autophagy induction in tumor surrounding cells promotes tumor growth in adult *Drosophila* intestines. Dev. Biol. *476*, 294–307.

Stem Cell Reports, Volume *18*

Supplemental Information

A feedforward loop between JAK/STAT downstream target p115 and STAT in germline stem cells

Ruiyan Kong, Juan Li, Fuli Liu, Yankun Ma, Hang Zhao, Hanfei Zhao, Meifang Ma, and Zhouhua Li

Supplemental Information

1. SUPPLEMENTAL FIGURES

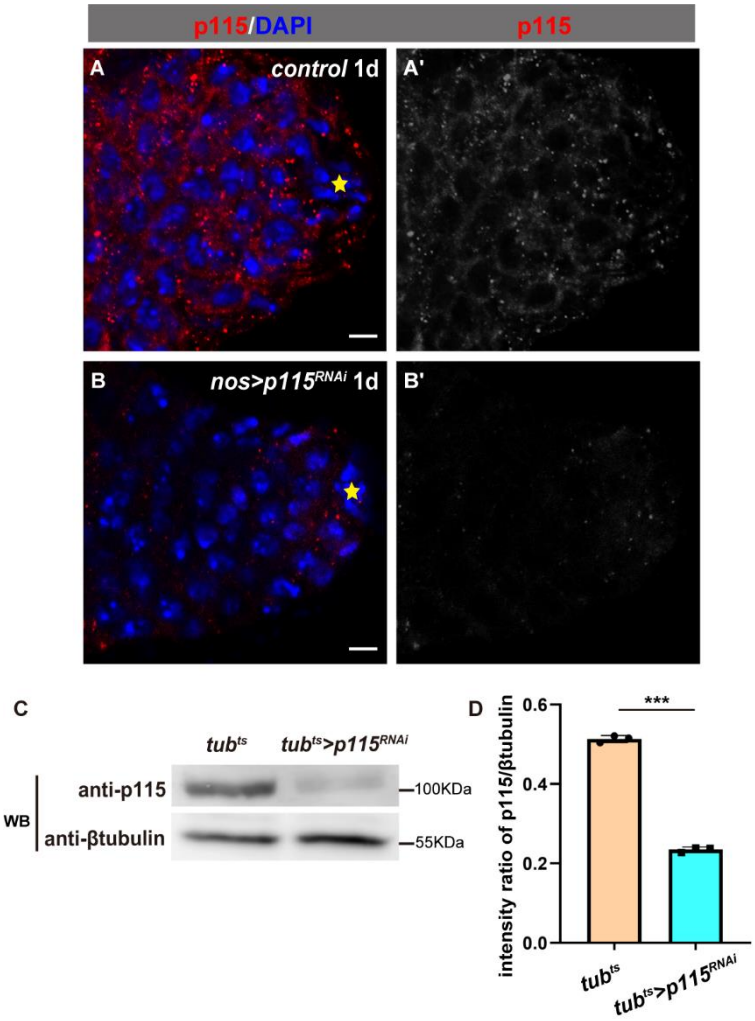

Figure S1. Knockdown efficacy of *p115*^{RNAi} and specificity of p115 antibody.

(A) Anti-p115 (red) staining in control showed p115 is mainly expressed in the cytoplasm as puncta. p115 channel is showed separately in black white.

(B) Knockdown of *p115* in germ cells significantly decreased the protein levels of p115 compared to those of control (A). p115 channel is showed separately in black white. The hubs are indicated by asterisks. Scale bars: 5 μm.

(C) Western blot analysis of p115 and βtubulin levels in lysate from control (*tub*^{ts}) and

tub^{ts} > *p115*^{RNAi}.

(D) Quantification of the ratio of p115/βtubulin from flies with indicated genotypes. Mean ± SD is showed. n=3. ***$P < 0.001$.

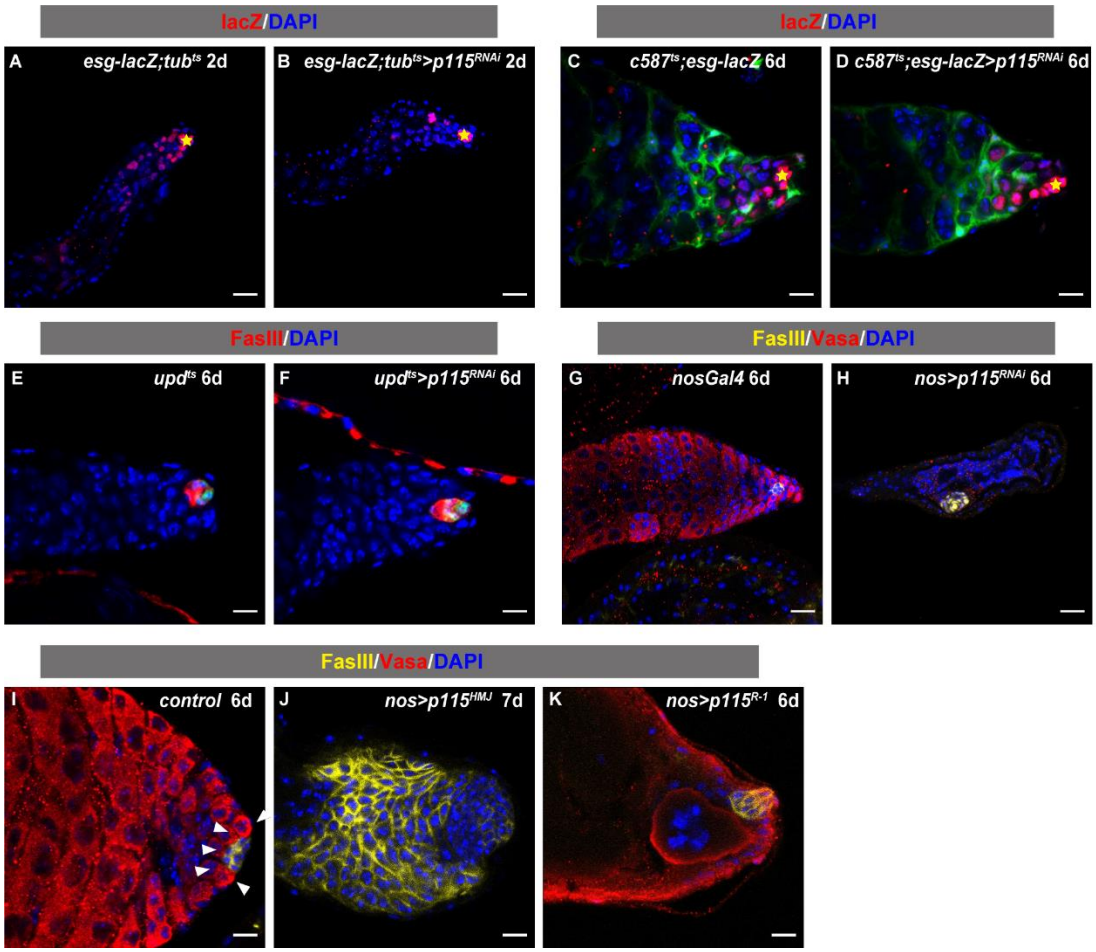

Figure S2. p115 functions in germline cells of adult testis.

(A and B) Systemic knockdown of *p115* using *esg-lacZ; tub*^{ts} led to dramatic reduction of *esg*$^{+}$ cells (*esg-lacZ* in red) (B) compared to control (A). The asterisk denotes the hub.

(C and D) Knocking down of *p115* in somatic cyst cell lineage using *c587Gal4, UAS-GFP, tubGal80*^{ts}*; esg-lacZ (c587*^{ts}*; esg-lacZ)* did not result in obvious defects in testis (*esg-lacZ* in red). The hub is marked by the asterisk.

(E and F) Knocking down of *p115* in the hub using *updGal4, UAS-GFP, tubGal80^{ts} (upd^{ts})* did not cause obvious changes (FasIII in red).

(G and H) Knocking down of *p115* in germline cell lineage using *nosGal4* led to germline cell loss at room temperature 6 d after eclosion.

(I-K) Knocking down of *p115* in germline cells by different RNAi constructs, *p115^{HMJ}* (J) and *p115^{R-1}* (K), caused germline cell loss (red) compared to control (I) (GSCs are indicated by white arrowheads).

Vasa is stained for germline cells, FasIII is stained for the hub, and DAPI is stained for the nucleus. *esg* is highly expressed in the hub and early germ cells. Scale bars: 10 μm (C-F, I-K) and 20 μm (A-B, G-H).

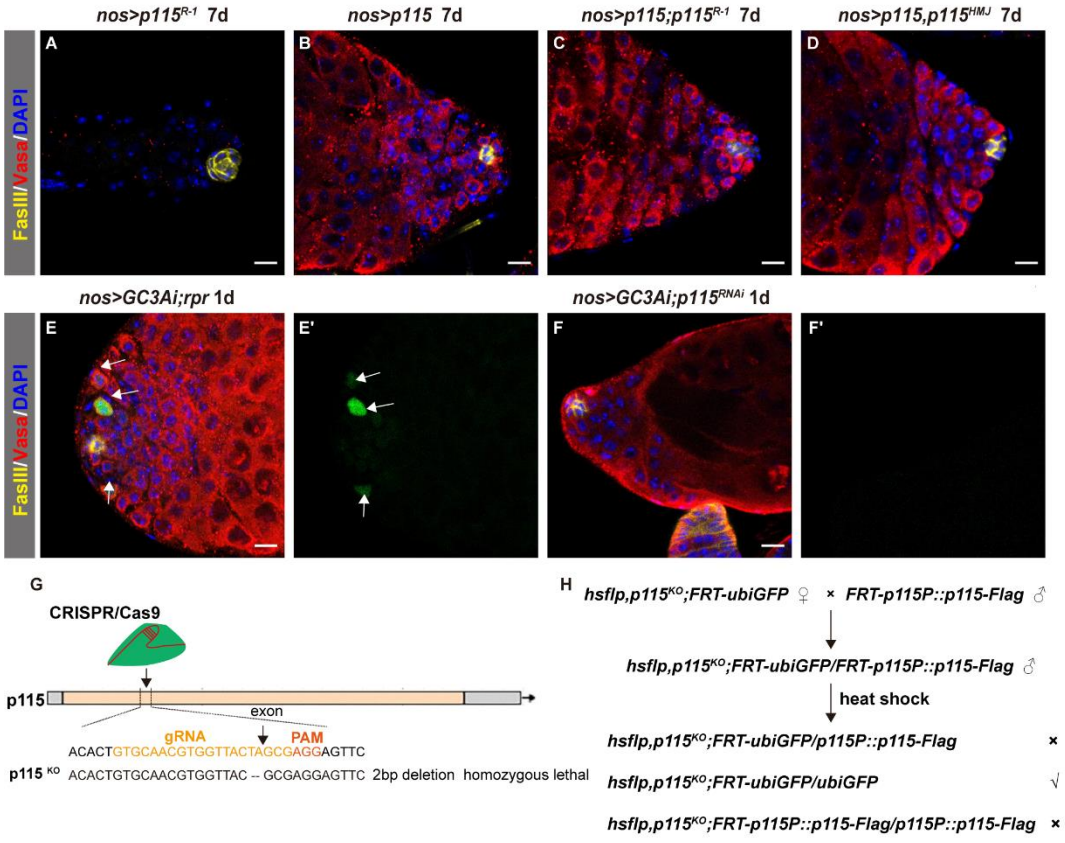

Figure S3. p115 is required for male GSC maintenance.

(A) The germline cells (red by Vasa) in *nos* > $p115^{RNAi}$ adult testis were totally lost at 7 d after eclosion. Please refer to Figures S2I and 2A for control.

(B) Overexpression of *p115* in germline cells results in no obvious phenotype. Please refer to Figure 2A for control.

(C and D) Overexpression of *p115* fully rescued the defects observed in *nos* > $p115^{RNAi}$ testes.

(E) Apoptosis (by GC3Ai in green) could be detected in germline cells expressing *reaper* (*rpr*) (white arrows).

(F) No apoptosis was detected in germline cells in *nos* > $p115^{RNAi}$ testes for 1 d.

(G) Diagram of $p115^{KO}$ mutant generated by CRISPR/Cas9. gRNA and PAM (protospacer adjacent motif) in capital letters are highlighted in light and dark brown, respectively. A 2 bp deletion was generated within gRNA target site in the coding exon of *p115*. Deletion is represented by a dash. $p115^{KO}$ mutant is homozygous lethal.

(H) The workflow to generate mosaic GSC clones of $p115^{KO}$ mutant. $p115^{KO}$ mutant mosaic clones were identified by stronger GFP signals than the neighboring cells (two copies of Ubi-GFP (homozygous $p115^{KO}$ mutant cells) vs one copy/none of Ubi-GFP (heterozygous $p115^{KO}$ mutant cells)).

Vasa is stained for germline cells, FasIII is stained for the hub, and DAPI is stained

for the nucleus. Scale bars: 10 μm.

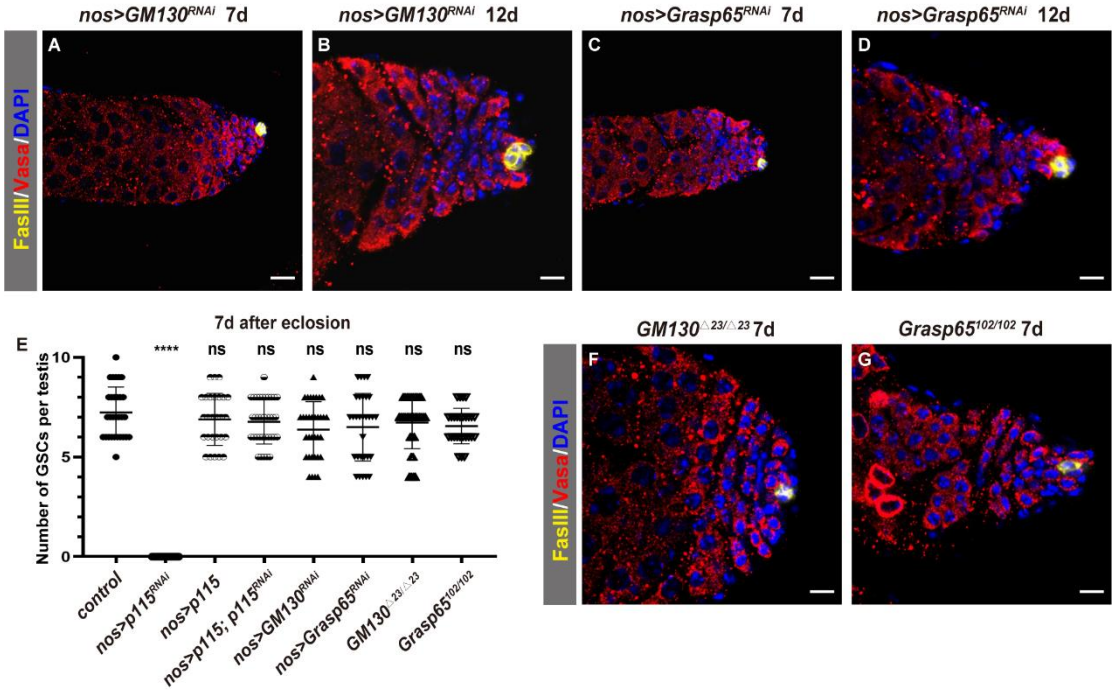

Figure S4. GM130 and Grasp65 are dispensable for male GSC maintenance.

(A and B) No obvious defects were observed in *nos > GM130*^{RNAi} testes at 7 d (A) and 12 d after eclosion (B). Please refer to Figure 2A for control.

(C and D) Knockdown of *Grasp65* in germline cells resulted in no obvious defects at 7 d (C) and 12 d after eclosion (D).

(E) Quantification of the number of GSCs in testes with indicated genotypes from 7-day-old animals (n=30 testes for *nosGal4* as control, n=21 for *nos > p115*^{RNAi}, n=28 for *nos > p115*, n=35 for *nos > p115; p115*^{RNAi}, n=34 for *nos > GM130*^{RNAi}, n=30 for *nos > Grasp65*^{RNAi}, n=33 for *GM130*$^{\Delta 23/\Delta 23}$, n=28 for *Grasp65*$^{102/102}$).

(F and G) No obvious defects were observed in *GM130* and *Grasp65* homozygous mutants. Mean ± SD is showed. Ordinary one-way ANOVA test was used, ns: not significant, ****P<0.0001.

Vasa marks germline cells, FasIII is stained for the hub, and DAPI is stained for the nucleus. Scale bars: 10 μm (B, D, F, G); 20 μm (A, C).

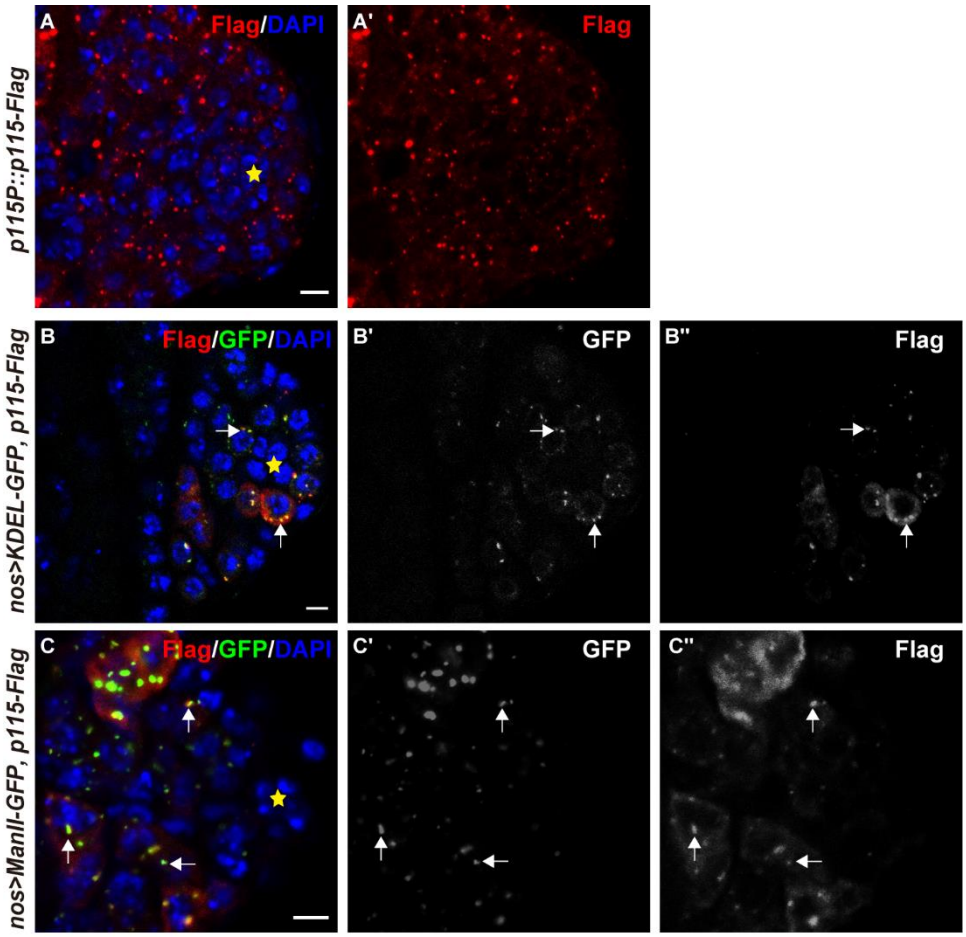

Figure S5. p115 mainly localize in cytosol, the ER and Golgi apparatus.

(A) Expression pattern of p115 is showed by anti-Flag (red) in *p115P::p115-Flag* testis. p115 is mainly expressed in the cytosol as punctate form. The hub is indicated

by asterisk. Flag channel is showed separately.

(B) Anti-Flag (red) and GFP (green) double labeling of *nos > KDEL-GFP, p115-Flag* testis showed co-localization of p115 and the ER (by KDEL-GFP, white arrows). KDEL-GFP and p115-Flag channels are showed separately in black white.

(C) Anti-Flag (red) and GFP (green) double labeling of *nos > Man II-GFP, p115-Flag* testis showed partial co-localization of p115 and the Golgi (by Man II-GFP, white arrows). Man II-GFP and p115-Flag channels are showed separately in black white.

Scale bars: 10 μm (A); 5 μm (B-C).

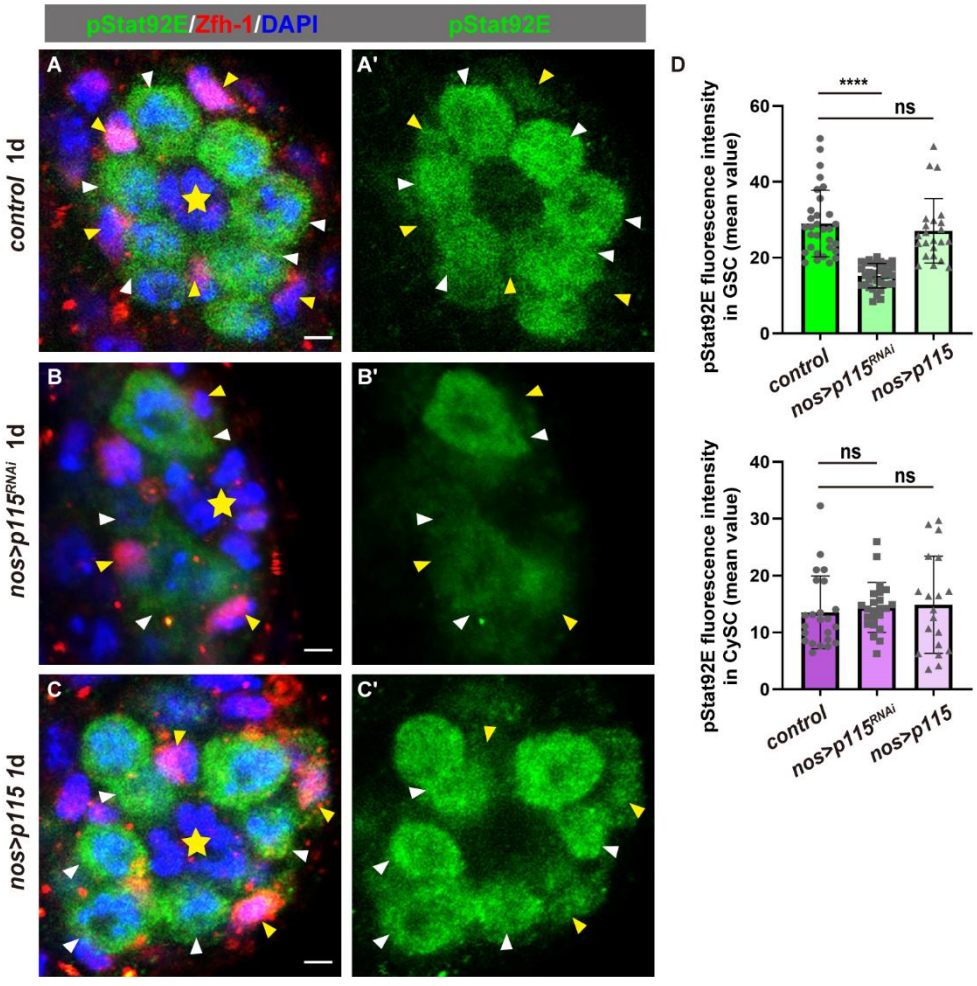

Figure S6. Depletion of p115 in GSCs significantly reduced the pStat92E levels in

GSCs but not in CySCs.

(A-C) Control, *nos > p115*^{RNAi}, and *nos > p115* testes were stained with anti-Zfh-1 antibody (red) to label CySCs and anti-pStat92E (green) antibody to label GSCs. GSCs are indicated by white arrowheads and CySCs are indicated by yellow arrowheads. The hubs are indicated by asterisks. The levels of pStat92E are significantly reduced in *p115*-depleted GSCs. Scale bars: 10 μm.

(D) Quantification of the levels of pStat92E in GSCs and CySCs in testis with indicated genotypes. Mean ± SD is showed. n ⩾ 15. ns, not significant, ****P<0.0001.

2. SUPPLEMENTAL EXPERIMENTAL PROCEDURES

Fly lines and cultures

Flies were maintained on standard diet 25°C with a 12 h/12 h light/dark cycle. The crosses were raised at 18°C and the desired hatched flies were picked up and transferred to new vials with fresh food every day at proper temperature and dissected at time points. Detailed information of the fly stocks used in this study can be found either in FlyBase or as noted: *FRT82B*, *esg-lacZ* (*M5-4*), *nosGal4*, *c587Gal4*, *UAS-GFP, tubGal80*^{ts}*; esg-lacZ (c587*^{ts}*; esg-lacZ)*, *UAS-hop*$^{Tum-l}$, *UAS-Dam* (a generous gift from Dr Andrea H. Brand) (Southall et al., 2013), *updGal4, UAS-GFP, tubGal80*^{ts} *(upd*^{ts}*)*, *esg-lacZ; tubGal4, tubGal80*^{ts} (*esg-lacZ; tub*^{ts}), *p115*$^{R-1}$ (NIG.1422R-1), *p115*^{HMJ} (HMJ23695), *GM130*^{RNAi} (NIG.11061R-1), *Grasp65*^{RNAi} (BL34082/HMS01093), *GM130*$^{\Delta 23}$ (BL65255), *Grasp65*^{102} (BL65257), *Stat92E-Flag-GFP* (BL38670), *UAS-HA-Stat92E* (a generous gift from Dr Erika A. Bach) (Ekas et

al., 2006), *UAS-KDEL-GFP* (BL9898), *UAS-rpr, nosGal4;UAS-GC3Ai* (BL84308), *UAS-Man II-GFP* (a generous gift from Dr Zhou Wei), *hsflp; FRT82B-ubiGFP* was used for mosaic clonal analysis. *w* (*white*) ^{RNAi} (BL33623) and/or $Gal4^{RNAi}$ (HMS504, from TRiP at Harvard Medical School) were used as control.

RNAi knockdown and overexpression experiments

Knockdowns and overexpression were performed by combining the *UAS-shRNA* fly lines and transgenic stocks respectively with *nosGal4*, upd^{ts}, $c587^{ts}$ or tub^{ts} drivers. Crosses were maintained at 18°C. Flies with desired genotype were collected and maintained at 18°C upon eclosion or transferred to 29°C according to experiment need. Flies were transferred to new vials with fresh food every day and dissected at time points. Please note that when the transgene is driven by *nosGal4* in the germline cells, the transgene is not equally expressed in all the germline cells.

Generation of transgenic flies

To identify JAK/STAT signaling downstream targets, *attB-UAST-STAT-Dam* was constructed. *STAT* ORF was amplified from *UAS-HA-Stat92E* (a generous gift from Dr Erika A. Bach) (Ekas et al., 2006) using primer pair (*STAT-Dam*-F:gatctggccggcgc AGATCTGCGGCCGCtcATGAGCTTGTGGAAGCGCATCGCCAGCC and *STAT-Dam*-R: gtaaggttccttcacaaagatccTCTAGATCAAAAGTTCTCAAAGtTTGTAATCGT ATC) and cloned into the NotI and XbaI sites of *attB pUAST-LT3-Dam* (a generous gift from Dr Andrea H. Brand) (Southall et al., 2013). To explore p115 function, two

pairs of oligoes were synthetized (*p115*-F1: ctagcagtGGAGAGCTTCTGTAGCA AACTtagttatattcaagcataAGTTTGCTACAGAAGCTCTCCgcg and *p115*-R1: aattcgc GGAGAGCTTCTGTAGCAAACTtatgcttgaatataactagTTTGCTACAGAAGCTCTCC actg. *p115*-F2: ctagcagtGGAGATGTTCATCAAGACACCtagttatattcaagcataGGTGTC TTGATGAACATCTCCgcg and *p115*-R2: aattcgcGGAGATGTTCATCAAGACACC tatgcttgaatataactaGGTGTCTTGATGAACATCTCCactg). The oligoes were annealed and cloned into the EcoRI and NheI sites of an *attB-pWALIUM20* vector (TRiP) to generate *attB-UAS-p115*^{shRNA}. *UAST-p115-Flag* construct was constructed by cloning the *p115* ORF amplified from gDNA using primer pair (*p115*-ERI-5': CTGAATAGG GAATTGGGAATTCatggagttcctgaagagtggcat and *p115*-ERI-3': CATTTTGGTAC GCCGGAATTCcctgctggcggtgccacttgg) into the EcoRI site of *attB-pUAST-nFlag* vector. *p115P::p115-Flag* was constructed by cloning the promoter and the coding region of *p115* from gDNA using primer pair *p115p*-ERI-5': CTGAATAGGGAATTGGGAATTCggcacacctgaagcgcccggc and *p115p*-ERI-3': CATTTTGGTACGCCGGAATTCcctgctggcggtgccacttggg into the EcoRI site of *attB-pUAST-nFlag* vector. *UAST-Stat92E-Flag-GFP* was constructed by cloning the Stat92E ORF from *UAS-HA-Stat92E* (from Erika A. Bach) (Ekas et al., 2006) using primer pair *STAT*-ERI-5': CTGAATAGGGAATTGGGAATTCatgagcttgtggaagcgcatct cc and *STAT*-XhoI-3': CGCCCTTGCTCACCATCTCGAGAAAGTTCtcaaagtttgtaatc gtatcgaagtcc into the EcoRI and XhoI site of *attB-pUAST-Flag-GFP* vector. Transgenic flies were obtained by standard P-element-mediated germline transformation carrying *attP* site at 86F.

Generation of *p115* knockout mutant

p115 knockout mutant was generated by CRISPR-Cas9 technology. *p115* guide RNA construct was generated by cloning the *p115* guide RNA into the BbsI site of *pCFD4* using primer pair *p115*-sgRNA1-F1: TATATAGGAAAGATATACCGGGTGAACTTC gtgcaacgtggttactagcgGTTTTAGAGCTAGAAATAGCAAG and *p115*-sgRNA1-R1: ATTTTAACTTGCTATTTCTAGCTCTAAAACcgctagtaaccacgttgcacGACGTTAAAT TGAAAATAGGTC. *p115* knockout mutant were generated by injecting *pCDF4-p115-sgRNA* vector into transgenic flies carrying Cas9 protein. The mutants were identified by PCR using primer pair *p115*-KO1-F: GCACCAGGGCTGTCGAGTCGT and *p115*-KO1-R: TTGGATGTTTGAGTTGCCCTTGGTC. PCR products were sequenced to determine the deleted regions.

Mosaic clone analyses

Clones were generated using FLP/FRT system-mediated mitotic recombination. Flies with genotype of *hsflp; FRT82B-ubiGFP* or *hsflp, $p115^{KO}$; FRT82B-ubiGFP* were crossed with flies with genotype of *FRT82B* or *FRT82B-p115P::p115-Flag*. Males with the desired genotypes were selected to conduct time-course clonal analysis after clone induction (ACI). GSC clones were induced by heat shocking two-day-old males with desired genotypes 1 hour at 37°C, twice a day for 2 days. The heat shock-treated flies were maintained at 22°C and transferred to new vials with fresh food daily before dissection.

Generation of mouse anti-p115 antibody

A GST fusion protein containing the region of p115 (101-301 aa) with a GST tag at its N terminal was used as antigen. A DNA fragment encoding 101-301 aa of p115 was amplified and cloned into the BamHI and EcoRI sites of *pGEX-4T-1* vector using primers: *GST-p115*-5': CGGATCTGGTTCGCGTGGATCCgaggaggctgataatcccaccg and *GST-p115*-3': GCTCGAGTCGACCCGGGAATTCctactgattactggagttgttcttg. Fusion proteins were purified according to the manufacturer's protocol and mice were immunized following standard procedure.

Immunostaining and imaging

Testes were dissected in 1×PBS buffer and fixed in 4% PFA for 20 minutes at room temperature. The samples were then rinsed, washed with 1×PBT (0.1% Triton X-100 in 1×PBS) three times, one time for 5mins and blocked in 3% BSA in 1×PBT for 45 min. The samples were then incubated with primary antibodies at 4°C overnight. The following primary antibodies were used: rabbit anti-Zfh-1 (1:50,000) (Xu et al., 2018), rabbit anti-Vasa (d-260, 1:200, Cat No: sc-30210, Santa Cruz, USA), rabbit anti-Vasa (1:2,000) (Zhao et al., 2022), mouse anti-α-Spectrin (3A9, 1:50, developed by D. Branton, and R. Dubreuil, Developmental Studies Hybridoma Bank (DSHB)), mouse anti-FasIII (7G10, 1:100, developed by C. S. Goodman, DSHB), rabbit anti-GFP (1:1,000, Abcam, USA), mouse anti-γ-tubulin (1:1,000, Abbkine, USA), guinea pig anti-Stat92E (1:1,000, a generous gift from Dr Yu Cai), mouse anti-pStat92E (1:2,000,

Abmart, China)(Zhang et al., 2013), rabbit anti-β-glactosidase (lacZ, 1:5,000, Cat No: 55978, Cappel, USA), mouse anti-Flag (1:2,000, Sigma-Aldrich, USA). The rinsing and washing procedures were conducted and samples were then incubated with the secondary antibodies conjugated with Cy3, 488, or Cy5 (Jackson ImmunoResearch, USA) with a dilution of 1:400 for 2 h at room temperature. DAPI (Sigma, 0.1 μg/ml) was added to the secondary antibodies staining. All images were captured using Zeiss LSM 780 laser scanning confocal microscope and processed in Adobe Photoshop and Illustrator.

Transmission electron microscopy

The testes were dissected and fixed in cold 2.5% glutaraldehyde (stored at 4°C), and then washed 4 times with PB buffer (0.1 M). The tissue underwent post-fixation with Osmium tetroxide (1%) and Tetra potassium hexacyanoferrate trihydrate (1.5%) for 1 h at 23℃, followed by ethanol dehydration in graded solutions (50%, 70%, 80%, 90%, 100%, 100%, 100%) for 5min each. Then, 1, 2-Epoxypropane twice for 5min each and gradient infiltration with mixture of 1, 2-Epoxypropane and Epon 812 resin for 8 h (SPI, America). Subsequently, Pure Epon 812 twice and polymerizing in oven (60°C). Blocks of polymerized resin were sectioned using a Leica EM UC7 ultramicrotome (Wetzlar, Germany). Ultra-thin sections (70 nm) were mounted and dried on coated copper grids. Sections were stained on-grid with 2% uranyl acetate (25 min) and lead citrate (5 min). Imaging was carried out using H-7650B transmission electron microscope (Hitachi, Tokyo, Japan).

Quantitative real-time PCR

Total RNA was extracted from ~300 testes using TRIzol (Invitrogen, USA) and was cleaned using RNAeasy (QIAGEN, USA). Extracted total RNA was used to synthesize cDNA through GoTaq® qPCR Master Mix (PROMEGA, USA) according to the manufacturer's instructions. Oligo (dT)15 primer was used for cDNA library synthesis, which was then used for qPCR. NovoStart® SYBR qPCR SuperMix Plus (Novoprotein, China) was used to perform qPCR following the standard protocol provided by QuantStudio 7 Real-Time PCR System (Applied Biosystems, USA). qPCR was performed in duplicate for each of three independent biological replicates. All results are presented as mean ± SD of the biological replicates. Ribosomal gene *RpL11* was used as normalization control. P-values and data significance was calculated according to two-tailed Student's *t* test.

Dam-ID

Dam-ID was carried out according to a previously described method (Gutierrez-Triana et al., 2016). Testes from *c587^{ts};hop^{Tum-l},STAT-Dam* and *c587^{ts};hop^{Tum-l},UAS-Dam* (control) adult fly (about 2,000 flies) were collected after two days expression and immediately preserved on dry ice and kept at -80°C. Genomic DNA was then isolated and amplified as described in (Chen et al., 2018). Dam-ID sequence quality was examined by FastQC (version 0.11.9). Dam-ID-seq reads were aligned using Bowtie2 (version 2.5.0) to build version dm6 of the *D. melanogaster* genome.

MACS2 (version 2.2.7.1) was used to call peaks from alignment results and to identify regions of enrichment. BigWig files were generated for visualization using the bioconductor-chipseeker (Version 1.18.0). Raw data from the Dam-ID were submitted to Gene Expression Omnibus (http://ncbi.nlm.nih.gov/geo) with the access number GEO: GSE226582.

Co-Immunoprecipitation and western blotting

Fly tissues were lysed in RIPA buffer (50 mM Tris-HCl, pH 8.0, 150 mM NaCl, 5 mM EDTA, pH 8.0, 0.5% Triton X-100, 0.5% NP-40, 0.5% sodium deoxycholate, and complete protease inhibitor cocktail tablets (Roche, USA)) on ice for 30 minutes. After centrifugation (13,000 rpm,10 minutes at 4°C), lysates were then diluted ten-fold with RIPA buffer and subjected to immunoprecipitation using anti-Flag M2 affinity gel (A2220, Sigma-Aldrich, USA). The immunocomplexes were collected by centrifugation and washed with 1 ml of RIPA buffer three times, one time for 5 mins. For western blotting, immunoprecipitated proteins were separated in SDS-PAGE and then blotted onto PVDF membranes. The membranes were stained with the primary antibody overnight at 4°C. Followed by washing with 1×PBST (0.1% Tween 80 in 1×PBS), PVDF membranes were incubated with the secondary antibodies conjugated with HRP, then the membranes were scanned using Luminescent Image Analyzer (GE, Sweden). Mouse anti-p115 (1:1,000, this study), mouse anti-Flag (1:1,000, Sigma-Aldrich, USA), mouse anti-HA (1:1,000, Sigma-Aldrich, USA), mouse anti-βtubulin (1:1,000, Abbkine, USA) and guinea pig anti-Stat92E (1:1,000, a generous gift from

Dr Yu Cai) antibodies were used.

Signal quantification

Image J software was used for signal quantification (pStat92E and Stat92E). Two parameters, integrated optical density (IOD) and area, were used in the analysis. IOD value per cell was used. At least six different images were analyzed for each sample.

Data analysis

The number of GSCs or spectrosome-containing cells were counted from selected testes under a fluorescence microscope. The number of GSCs in testis was counted according to Vasa staining, α-Spectrin staining, and the position (GSCs are attached to hub cells). A marked GSC clone was calculated by carrying a $GFP^{+/+}$ cell attached to hub cells. The mean fluorescent intensity of Stat92E and pStat92E in GSCs and western blots blands grey values were measured by Image J software. Data processing was analyzed and performed using GraphPad Prism 7.0 (GraphPad Software Inc., USA). P values were determined by two-tailed Student's *t* tests or Ordinary one-way ANOVA test. ^{ns} P > 0.05; *P < 0.05; **P < 0.01; *** P < 0.001; ****P < 0.0001.

qRT-PCR primers used:

p115-S: CACCGCCAGCAGGTAGAAAT

p115-A: TTGCGATTTGCTGCAGTTCC

RpL11-S: GGTCCGTTCGTTCGGTATTCGC

RpL11-A: GGATCGTACTTGATGCCCAGATCG

3. SUPPLEMENTAL REFERENCES

Chen, J., Xu, N., Wang, C., Huang, P., Huang, H., Jin, Z., Yu, Z., Cai, T., Jiao, R., and Xi, R. (2018). Transient Scute activation via a self-stimulatory loop directs enteroendocrine cell pair specification from self-renewing intestinal stem cells. Nat Cell Biol *20*, 152-161.

Ekas, L.A., Baeg, G.H., Flaherty, M.S., Ayala-Camargo, A., and Bach, E.A. (2006). JAK/STAT signaling promotes regional specification by negatively regulating wingless expression in Drosophila. Development *133*, 4721-4729.

Gutierrez-Triana, J.A., Mateo, J.L., Ibberson, D., Ryu, S., and Wittbrodt, J. (2016). iDamIDseq and iDEAR: an improved method and computational pipeline to profile chromatin-binding proteins. Development *143*, 4272-4278.

Southall, T.D., Gold, K.S., Egger, B., Davidson, C.M., Caygill, E.E., Marshall, O.J., and Brand, A.H. (2013). Cell-Type-Specific Profiling of Gene Expression and Chromatin Binding without Cell Isolation: Assaying RNA Pol II Occupancy in Neural Stem Cells. Developmental Cell *26*, 101-112.

Xu, R., Li, J., Zhao, H., Kong, R.Y., Wei, M., Shi, L., Bai, G., and Li, Z.H. (2018). Self-restrained regulation of stem cell niche activity by niche components in the Drosophila testis. Developmental Biology *439*, 42-51.

Zhang, Y., You, J., Ren, W., and Lin, X. (2013). *Drosophila* glypicans Dally and Dally-like are essential regulators for JAK/STAT signaling and Unpaired distribution in eye development. Dev Biol *375*, 23-32.

Zhao, H., Li, Z.R., Kong, R.Y., Shi, L., Ma, R., Ren, X.J., and Li, Z.H. (2022). Novel intrinsic factor Yun maintains female germline stem cell fate through Thickveins. Stem Cell Rep *17*, 1914-1923.